Norwegian
Meteorological
Institute

No. 10/2022
ISSN 2387-4201
Sea ice/Ice
service

METreport
User Guide for Multi-Sensor Ice Analysis Data

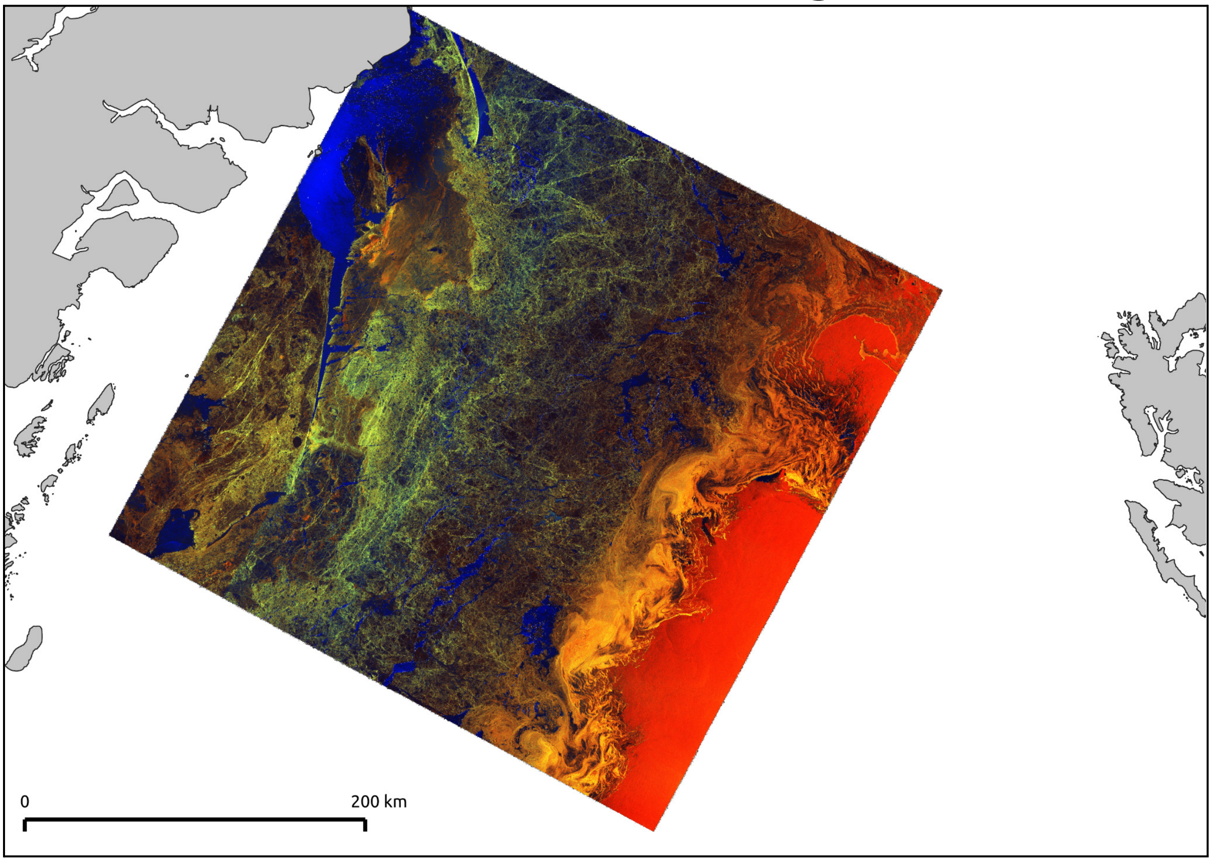

Analysis for Belgica Bank, North East Greenland 2019-20

Frank Andreas Amdal, Nick Hughes

Classification: open

Title User Guide for Multi-Sensor Ice Analysis Data: Analysis for Belgica Bank, North East Greenland 2019-20	**Date** 2022-09-08
Section Ice Service	**Report no.** No. 10/2022
Author(s) Frank Andreas Amdal, Nick Hughes	**Classification** ● Free ○ Restricted
Client(s) EU H2020, ESA	**Client's reference** H2020 825258, ESA 4000130509/20/NL/FF/ab

Abstract

This report consists of two parts:

The first part describes the data sources, nomenclature, file formats and data in the analysis. The intention is that this dataset can be used for machine learning and deep neural network training/validation, and it distinguishes sea ice concentration, type and form derived from a combination of different satellite sensors including ALOS-2, Sentinel-1, COSMO-SkyMed, Sentinel-2, and ICESAT-2. The region chosen for the analysis was the Belgica Bank area offshore of North East Greenland, as this is an area which experiences a wide variety of sea ice, and iceberg, conditions throughout the year. The dataset consists of two parts: 11 days of individual sea ice interpretations, one for each month in the period from April 2019 to March 2020, with the exception of October 2019, and iceberg surveys derived from Sentinel-2 for spring in 2019 and 2020.

The second part of this report compares synthetic aperture radar (SAR) data from both L-band ALOS-2 and C-band Sentinel-1 satellites, and identifies the visible synergies and anomalies. The results confirm that there are variations in backscatter signatures between ALOS-2 and Sentinel-1 data when comparing them for different sea ice situations and conditions. ALOS-2 data in many cases is proven to be a reliable and beneficial source of data when it comes to identifying icebergs, ridges, determining sea ice type, and also distinguishing ice and water compared to standalone Sentinel-1 data.

The data can be accessed at https://zenodo.org/record/7053975.

Keywords

Sea Ice, Icebergs, Sentinel-1, ALOS-2, COSMO-SkyMed, Sentinel-2, ICESat-2

Disciplinary signature

Responsible signature

Meteorologisk institutt
Meteorological Institute
Org.no 971274042
post@met.no

Oslo
P.O. Box 43 Blindern
0313 Oslo, Norway
T. +47 22 96 30 00

Bergen
Allégaten 70
5007 Bergen, Norway
T. +47 55 23 66 00

Tromsø
P.O. Box 6314,
Langnes
9293 Tromsø, Norway
T. +47 77 62 13 00

www.met.no

Table of Contents

List of Figures

List of Tables

Meteorologisk institutt
Meteorological Institute
Org.no 971274042
post@met.no

Oslo
P.O. Box 43 Blindern
0313 Oslo, Norway
T. +47 22 96 30 00

Bergen
Allégaten 70
5007 Bergen, Norway
T. +47 55 23 66 00

Tromsø
P.O. Box 6314,
Langnes
9293 Tromsø, Norway
T. +47 77 62 13 00

www.met.no

1. Introduction

This report is intended as a user guide to the sea ice and iceberg classification dataset produced as part of the work of the Centre for Integrated Remote Sensing and Forecasting for Arctic Operations (CIRFA)[1] in the European Horizon 2020 "*From Copernicus Big Data to Extreme Earth Analytics*" (ExtremeEarth)[2] and ESA "*Synergistic Use of L- and C-Band SAR Satellites for Sea Ice Monitoring*"[3] projects. The data can be accessed at https://zenodo.org/record/7053975.

The dataset consists of manual sea ice analysis derived from 11 different months, from April 2019 to March 2020, and iceberg surveys for the spring of 2019 and 2020, for the area offshore of the North East Greenland coastline covering the Belgica Bank (Figure 1).

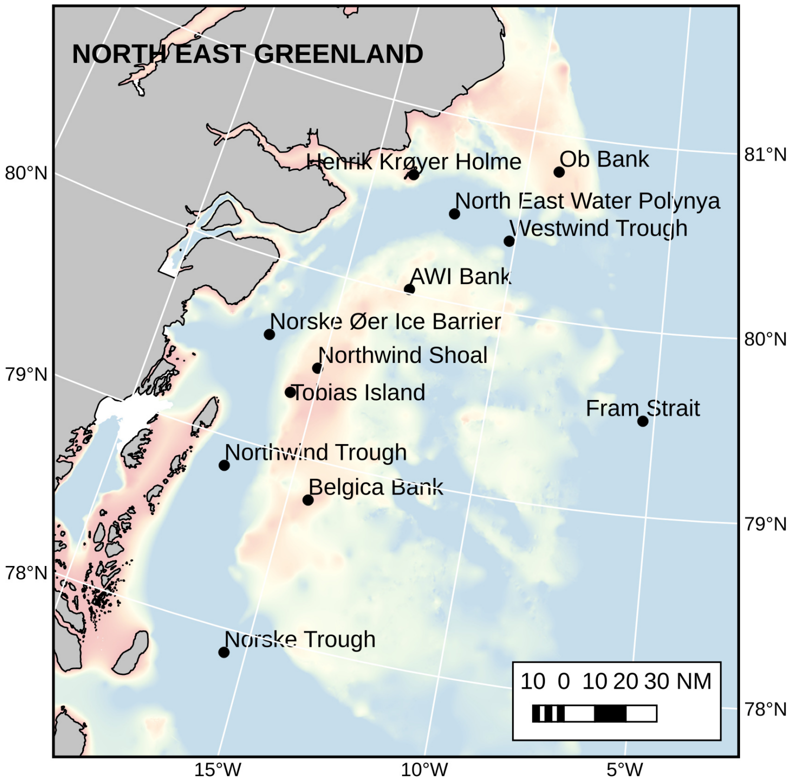

Figure 1: Map of the Belgica Bank area showing key locations in this report.
Bathymetry from the International Bathymetric Chart of the Arctic Ocean (IBCAO) [Jakobsson et al, 2020]

The region experiences a wide variety of sea ice conditions and has a large number of icebergs. A key feature is the formation of an extensive (land)-fast ice fringe along the coast in the winter that is anchored by grounded icebergs. This incorporates different ice types, including from new ice being grown in situ and multi-year ice that has drifted into the area. The fast ice is known as the Norske Øer Ice Barrier (NØIB)

---

[1] CIRFA is one of 17 Centres for Research-based Innovation (SFI) granted in 2014 and is funded under the Research Council of Norway (RCN) project number 237906

[2] The ExtremeEarth project received funding from the European Union's Horizon 2020 research and innovation programme under grant agreement No. 825258.

[3] ESA Contract No. 4000130509/20/NL/FF/ab

(Hughes and others, 2011) and is typically bordered to the north by the open water of the North East Water (NEW) polynya (Schneider and Budéus, 1997). This is an example of a latent heat polynya, more typically found around the Antarctic continent, formed by winds and currents pushing the sea ice away from the coast and fast ice edge. This, and other latent heat polynyas, are key areas for sea ice formation, Offshore of the fast ice is the more variable, drift ice cover transiting southward on the East Greenland Current (EGC).

Because the fast ice remains in place for a large part of the year, it is ideal for remote sensing studies as conditions can be interpolated between satellite data acquisitions without having to factor in ice drift. The wide range of ice conditions on Belgica Bank make it an ideal test laboratory for comparing the response of different sensors throughout the full seasonal cycle, and for calibration and validation of new classification algorithms.

In this report we first describe the different data sources used, the data format including nomenclature, the content of the dataset, and finally a comparison of the sea ice observing capabilities of L- and C-band SAR sensors. The dataset is intended for calibration and validation of new satellite data classification algorithms. It intentionally does not include the satellite data, as the characteristics of this are heavily dependent on the pre-processing used, and it is impossible to include the full range of every type of satellite data available for the whole time period. In some cases, for example for ALOS-2 and COSMO-SkyMed, access to the raw source data is subject to end-user licensing and it is not open source.

2. Data Sources

The primary data source used for the manual classification is satellite data from L-band synthetic aperture radar (SAR), supplemented by C-band SAR from Sentinel-1, X-band SAR from COSMO-SkyMed, very high resolution optical data from Sentinel-2, and laser altimeter data from ICESat-2. In addition, meteorological data has been used to provide the context of prevailing environmental conditions.

2.1 ALOS-2

The Advanced Land Observing Satellite-2 (ALOS-2) operated by the Japan Aerospace Exploration Agency (JAXA) was launched 24 May 2014 and carries the Phased Array type L-band Synthetic Aperture Radar-2 (PALSAR-2) instrument that operates at 1.2 GHz.

For this study we used ScanSAR Wide images that cover a swath width of 490 km at a resolution of 60 m in dual (HH+HV) polarisation. The data was supplied in Level-1.5 GeoTIFF format as part of the European Space Agency (ESA) "*Synergistic Use of L- and C-Band SAR Satellites for Sea Ice Monitoring*" project[4] and Sections 5 and 6 of this report explore the synergies and differences in more detail. ScanSAR Wide images have an incidence angle range of 8-70° and have a Noise Equivalent Sigma Zero (NESZ) of -26 dB.

Other modes, including Spotlight and Stripmap are also available (Figure 2), as are a full and compact polarimetric capability, but were not explored in this study.

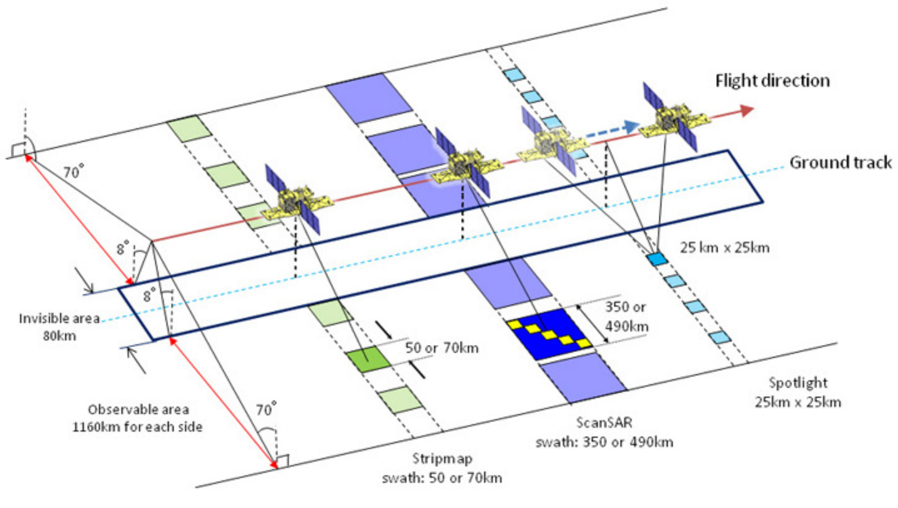

Figure 2: ALOS-2 acquisition modes.
[Image source: JAXA]

[4] ESA Contract No. 4000130509/20/NL/FF/ab

2.2 Sentinel-1

The Sentinel-1 mission is the European Radar Observatory for the Copernicus joint initiative of the European Commission (EC) and the European Space Agency (ESA) and consists of a constellation of two satellites sharing the same near polar orbital plane. The satellites carry identical C-band SAR instruments operating at 5.405 GHz that provide 4 operating modes; Stripmap (SM), Interferometric Wide Swath (IW), Extra Wide Swath (EW), and Wave (WV) (Figure 3). These can provide data as either single or dual polarisation, and for this study we used EW mode dual (HH+HV) polarisation with a 400 km swath at 40 m resolution as this is closest in specification to the ALOS-2 ScanSAR Wide mode and typically used for sea ice monitoring. These images have an incidence angle range of 20-46° and NESZ of -22 dB.

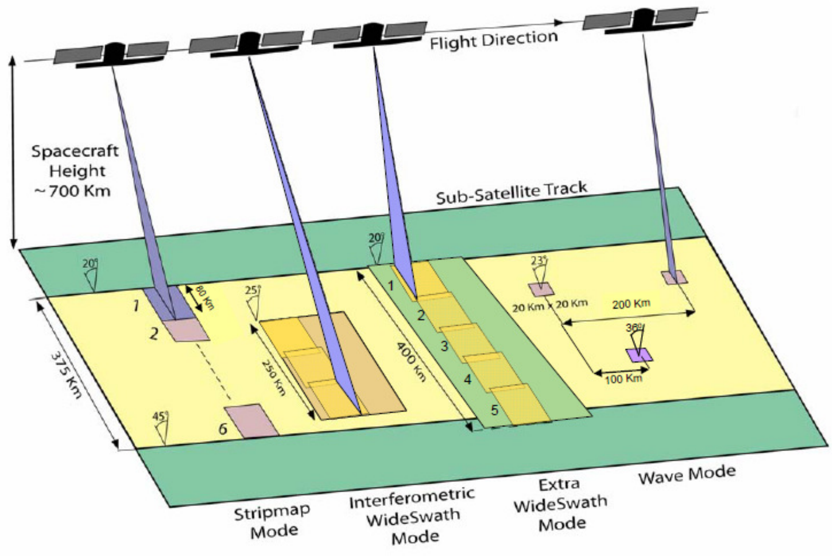

Figure 3: Sentinel-1 acquisition modes.
[Image source: ESA]

2.3 COSMO-SkyMed

COSMO-SkyMed is an Italian Earth-imaging constellation consisting of four identical high spatial resolution X-band (9.6 GHz) SAR satellites that have 5 operating modes; Huge Region and Wide Region which are both ScanSAR, Himage and Pingpong that are both Stripmap, and Mode-2 which is Spotlight (Figure 4). For this study we used Himage data with a 40 km swath at 2.5 m resolution acquired by ESA as part of the support for Copernicus services. These cover a smaller area south-east from Tobias Island (79°20'N 15°48'W) on Belgica Bank, to the usual fast ice edge. The first generation of satellites used in this study were launched between 23 June 2004 and 5 November 2010. A second generation of 4 satellites, with additional capabilities, started to be launched on 18 December 2019, and is expected to be completed in 2027.

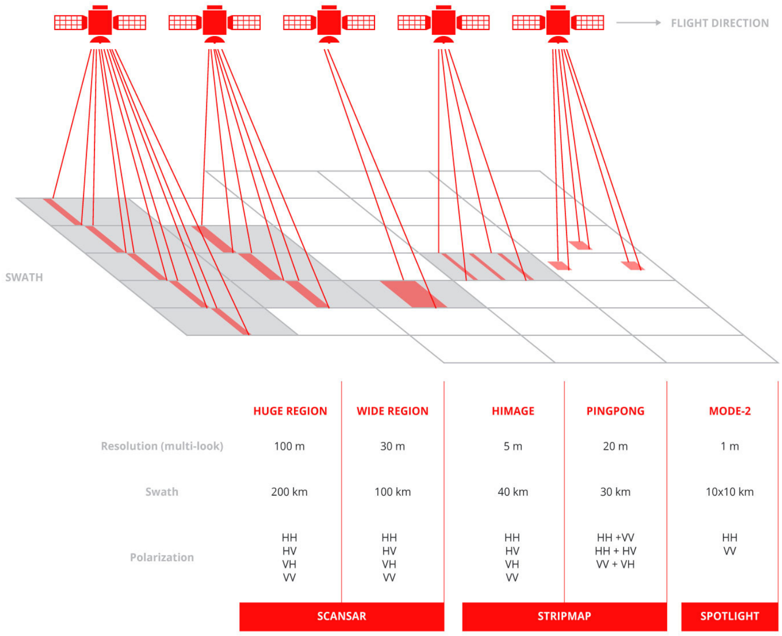

Figure 4: COSMO-SkyMed acquisition modes.
[Image source: e-Geos]

2.4 Sentinel-2

The Copernicus Sentinel-2 mission is based on a constellation of two twin near polar orbiting satellites which acquires wide-swath, high spatial resolution optical imagery. Each of the Sentinel-2 satellites carries a single payload of Multi-Spectral Instrument (MSI) that samples 13 spectral bands, four bands at 10 m, six bands at 20 m and three bands at 60 m spatial resolution. For Level-1C data the images are split into tiles of 100x100 km ortho-images in UTM/WGS84 projection (Figure 5).

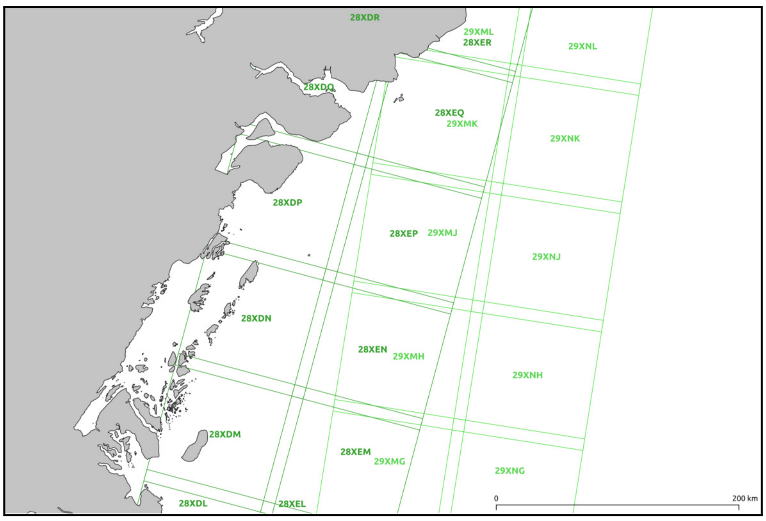

Figure 5:Sentinel-2 tiles over Belgica Bank.

2.5 ICESat-2

Ice Cloud and land Elevation Satellite-2 (ICESat-2) is part of NASA's earth science research, which focuses on how much our cryosphere is changing in a warming climate. The ICESat-2 was launched by NASA on September 15, 2018 into a near-circular, near-polar orbit. The satellite is equipped with a laser altimeter that uses individual photons to very precisely detect elevation with an accuracy of 4 mm at the earth's surface, and for our purpose the thickness of the ice. This provides 6 parallel beams, arranged in 3 groups of 2 (Figure 6).

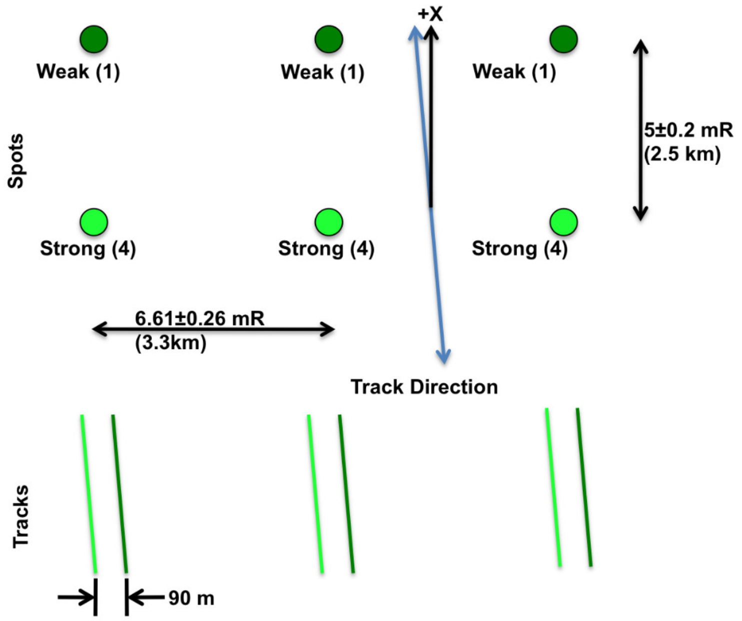

Figure 6: ICESat-2 beam pattern.
[Image source: NASA]

2.6 Weather Observations

The Norwegian Meteorological Institute in-house meteorological visualisation software Diana has been used to attain information about weather, temperature and wind conditions. The weather observations have mainly been derived from the Henrik Krøyer Holme weather station (Figure 7).

Meteorologisk institutt
Meteorological Institute
Org.no 971274042
post@met.no

Oslo
P.O. Box 43 Blindern
0313 Oslo, Norway
T. +47 22 96 30 00

Bergen
Allégaten 70
5007 Bergen, Norway
T. +47 55 23 66 00

Tromsø
P.O. Box 6314,
Langnes
9293 Tromsø, Norway
T. +47 77 62 13 00

www.met.no

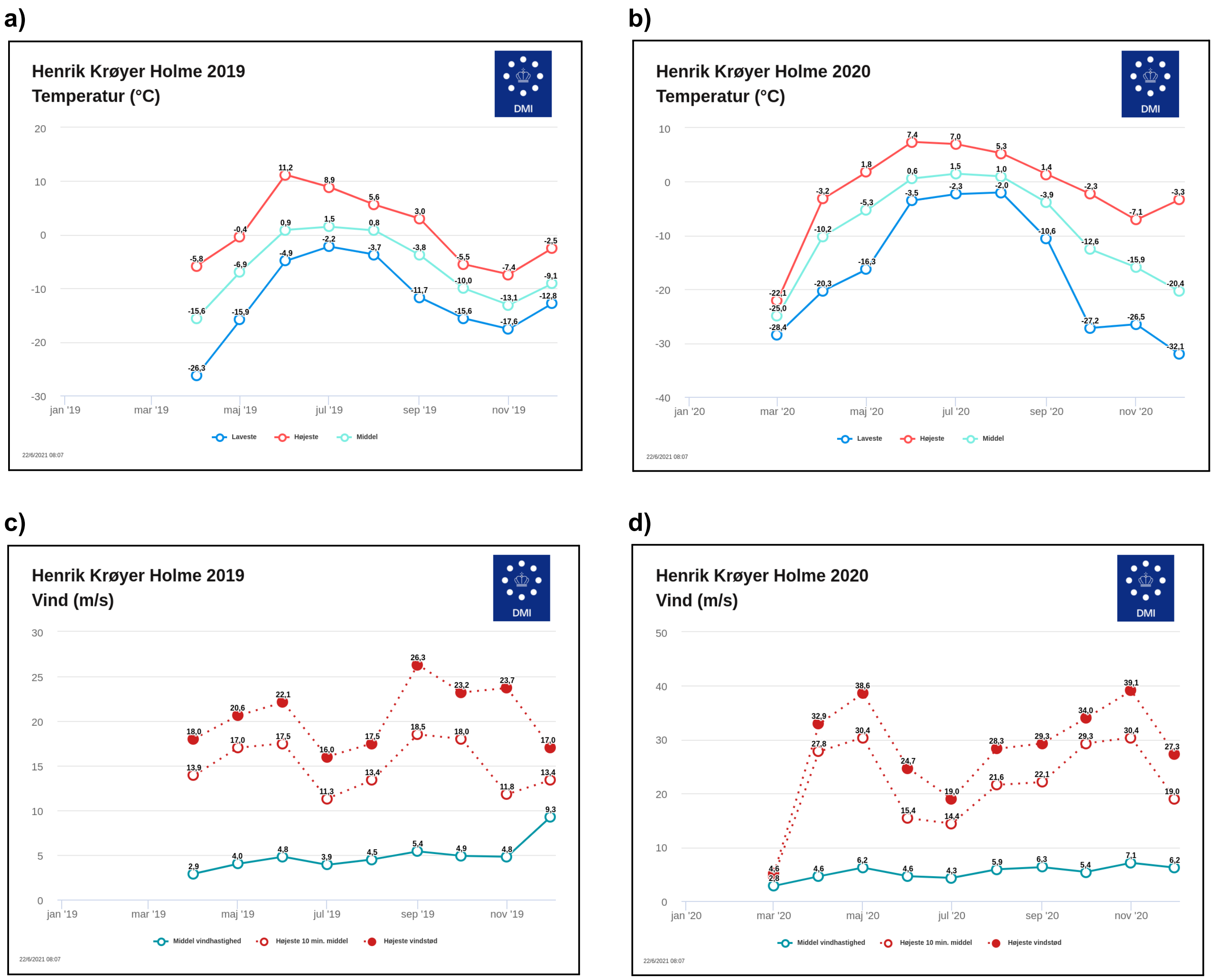

Figure 7: Time series of weather observations at the Henrik Krøyer Holme weather station. a) Temperature 2019. b) Temperature 2020. c) Wind 2019. d) Wind 2020.
[image source: DMI].

3. Data Format

3.1 Projection

The analysis Shapefiles are provided in the EPSG:3996 WGS84/IBCAO Polar Stereographic map projection. This is centred at 90° N and rotated to 0° E. The Well-Known Text (WKT) for this is:

```
PROJCS["WGS 84 / IBCAO Polar Stereographic",
    GEOGCS["WGS 84",
        DATUM["WGS_1984",
            SPHEROID["WGS 84",6378137,298.257223563,
                AUTHORITY["EPSG","7030"]],
            AUTHORITY["EPSG","6326"]],
        PRIMEM["Greenwich",0,
            AUTHORITY["EPSG","8901"]],
        UNIT["degree",0.0174532925199433,
            AUTHORITY["EPSG","9122"]],
        AUTHORITY["EPSG","4326"]],
    PROJECTION["Polar_Stereographic"],
    PARAMETER["latitude_of_origin",75],
    PARAMETER["central_meridian",0],
    PARAMETER["scale_factor",1],
    PARAMETER["false_easting",0],
    PARAMETER["false_northing",0],
    UNIT["metre",1,
        AUTHORITY["EPSG","9001"]],
    AXIS["X",EAST],
    AXIS["Y",NORTH],
    AUTHORITY["EPSG","3996"]]
```

The PROJ library (PROJ contributors, 2020) representation of this is:

```
+proj=stere +lat_0=90 +lat_ts=75 +lon_0=0 +k=1 +x_0=0 +y_0=0
+datum=WGS84 +units=m +no_defs
```

3.2 Sea ice

The training data has been interpreted in QGIS. The interpretation contains a subset of the information fields available in the full SIGRID-3 format, as listed in Table 1.

Table 1: Sea ice Shapefile data fields.

Field name	*Data type*	*Description*
ID	Integer	Identifier for each polygon
icetype	String	Single character string providing basic classification into: W = Open water (ice-free) I = Sea ice, fast ice, glacier ice or icebergs
si3ct	Integer	Total ice concentration, CA+CB, encoded as per SIGRID-3. See Table 2.
si3ca	Integer	Concentration of primary (thickest) ice type A, encoded as per SIGRID-3. See Table 2.
si3sa	Integer	Thickness of ice or stage of development for primary (thickest) ice type A, encoded as per SIGRID-3. See Table 3.
si3fa	Integer	Form of ice or floe size for primary (thickest) ice type A, encoded as per SIGRID-3. See Table 4.
si3cb	Integer	Concentration of secondary (thinnest) ice type B, encoded as per SIGRID-3. See Table 2.
si3sb	Integer	Thickness of ice or stage of development for secondary ice type B, encoded as per SIGRID-3. See Table 3.
si3fb	Integer	Form of ice or floe size for secondary (thinnest) ice type B, encoded as per SIGRID-3. See Table 4.
flag	integer	For labeling interesting features
comment	String	string providing information for that specific polygon.

Table 2: Ice concentration, as per SIGRID-3 Appendix E - Code Tables for SIGRID-3 Variables "Table 1: Concentration codes for variable identifiers CT, CA, CB, CC, AV, AK, AM and AT" (page 31)

Definition	*Code Figure*
Ice Free	98
Less than 1/10 (open water)	01
Bergy Water	02
1/10	10
2/10	20
3/10	30
4/10	40
5/10	50
6/10	60
7/10	70
8/10	80
9/10	90
10/10	92
Concentration intervals (lowest concentration in interval followed by highest concentration in interval)	
9/10 –10/10 or 9+/10	91
8/10 – 9/10	89
8/10 – 10/10	81
7/10 – 9/10	79
7/10 – 8 /10	78
6/10 – 8/10	68
6/10 – 7/10	67
5/10 – 7/10	57
5/10 – 6/10	56
4/10 – 6/10	46
4/10 – 5/10	45
3/10 – 5/10	35
3/10 – 4/10	34
2/10 – 4/10	24
2/10 – 3/10	23
1/10 – 3/10	13
1/10 – 2/10	12
Undetermined / Unknown	99

Meteorologisk institutt
Meteorological Institute
Org.no 971274042
post@met.no

Oslo
P.O. Box 43 Blindern
0313 Oslo, Norway
T. +47 22 96 30 00

Bergen
Allégaten 70
5007 Bergen, Norway
T. +47 55 23 66 00

Tromsø
P.O. Box 6314,
Langnes
9293 Tromsø, Norway
T. +47 77 62 13 00

www.met.no

Table 3: Ice type, as per SIGRID-3 Appendix E - Code Tables for SIGRID-3 Variables
“Table 2: Thickness of ice or stage of development codes for variable identifiers SA, SB, SC, CN, and CD.” (page 33)

Stage of Development	*Thickness*	*Code Figure*
Ice Free		01
Ice Thickness in cm	1-2 cm	02
	3 cm	03
	4 cm	04
	…	…
	50 cm	50
Ice Thickness interval, 5 cm	55 cm	51
	60 cm	52
	65 cm	53
	…	…
	95 cm	59
Ice Thickness interval, 10 cm	100 cm	60
	110 cm	61
	120 cm	62
	…	…
	190 cm	69
Ice Thickness interval, 50 cm	200 cm	70
	250 cm	71
	300 cm	72
	350 cm	73
Ice Thickness interval, 100 cm	00 cm	74
	500 cm	75
	600 cm	76
	700 cm	77
	800 cm	78
Brash Ice	Given by AV, AT, AM, AT	79

Table 3 continued: Ice type, as per SIGRID-3 Appendix E - Code Tables for SIGRID-3 Variables "Table 2: Thickness of ice or stage of development codes for variable identifiers SA, SB, SC, CN, and CD." (page 33)

Stage of Development	*Thickness*	*Code Figure*
No Stage of Development		80
New Ice	< 10 cm	81
Nilas, Ice Rind	< 10 cm	82
Young Ice	10 - <30 cm	83
Grey Ice	10 - <15 cm	84
Grey - White Ice	15 - <30 cm	85
First Year Ice	≥30 cm	86
Thin First Year Ice	30 - <70 cm	87
Thin First Year Stage 1	30 - <50 cm	88
Thin First Year Stage 2	50 - <70 cm	89
For Later Use		90
Medium First Year Ice	70 - <120 cm	91
For Later Use		92
Thick First Year Ice	≥120 cm	93
Residual Ice		94
Old Ice		95
Second Year Ice		96
Multi-Year Ice		97
Glacier Ice		98
Undetermined/Unknown		99

Notes:

a) This table has been extended to conform with the original SIGRID (1981) specification with two exceptions:
   - Code 01 has been used to represent Ice Free instead of an ice thickness of 1 cm. To conform with S-57 standards, code 00 is not used. There is little significant difference between an ice thickness of 1 cm and 2 cm.
   - Code 79 has been used for brash ice instead of a thickness of 900 cm as in the original SIGRID. The maximum ice thickness that can be reported by this code is therefore 800 cm instead of 900 cm.

b) To differentiate dark and light nilas gradations, use stage of development codes '03' and '07' respectively.

Meteorologisk institutt
Meteorological Institute
Org.no 971274042
post@met.no

Oslo
P.O. Box 43 Blindern
0313 Oslo, Norway
T. +47 22 96 30 00

Bergen
Allégaten 70
5007 Bergen, Norway
T. +47 55 23 66 00

Tromsø
P.O. Box 6314,
Langnes
9293 Tromsø, Norway
T. +47 77 62 13 00

www.met.no

Table 4: Form of ice or floe size, as per SIGRID-3 Appendix E - Code Tables for SIGRID-3 Variables "Table 13: Form of ice codes for variable identifiers FA, FB, FC, FP and FS." (page 35)

Form	*Size/Concentration*	*Code Figure*
Pancake Ice	30 cm - 3 m	22
Shuga/Small Ice Cake, Brash Ice	< 2 m across	01
Ice Cake	< 20 m across	02
Small Floe	20 m - <100 m across	03
Medium Floe	100 m - <500 m across	04
Big Floe	500 m - <2 km across	05
Vast Floe	2 km - <10 km across	06
Giant Floe	≥10 km across	07
Fast Ice		08
Growlers, Floebergs or Floebits		09
Icebergs		10
Strips and Patches	concentrations 1/10	11
Strips and Patches	concentrations 2/10	12
Strips and Patches	concentrations 3/10	13
Strips and Patches	concentrations 4/10	14
Strips and Patches	concentrations 5/10	15
Strips and Patches	concentrations 6/10	16
Strips and Patches	concentrations 7/10	17
Strips and Patches	concentrations 8/10	18
Strips and Patches	concentrations 9/10	19
Strips and Patches	concentrations 9+/10	91
Strips and Patches	concentrations 10/10	20
Level Ice		21
Undetermined/Unknown		99

4. Description of Data

The interpretation has been differentiated between water and ice, with polygons continuing under land areas. It is therefore recommended to apply a land mask layer in combination with the training data.

Values for sea ice concentration (CT, CA and CB), ice type (stage of development) (SA and SB), and form of ice (floe size) (FA and FB) are provided in the shapefiles attribute table.

As sea ice type is only subdivided into two classes with this interpretation setup there are some cases where there might be present three or more ice types within a polygon. In these cases only the two most prevalent stages of development have been prioritized.

For simplicity the stage of development interpretation for this training dataset has been subdivided into six categories:

> 81 - New ice: recently formed ice which includes frazil ice, grease ice and slush <=10cm.
> 82 - Nilas: thin elastic crust of ice, matt surface, <=10cm.
> 83 - Young ice: Transition stage between nilas and first-year ice, 10-30cm.
> 86 - First-year ice: Sea ice of not more than one winter's growth; 0,3 - 2m.
> 95 - Old ice: Has survived at least one summer's melt; <= 3m.
> 98 - Glacier ice: Ice of land origin, formed on land or in an ice shelf.
> 99 - Unknown

CA, SA and FA is the thickest/most developed ice type within the polygon.
CB, SB and FB is the second thickest/most developed ice type within the polygon.

In the areas where there is abundance of glacier and glacier ice, this ice type is labeled, but there are in some polygons a very small amount of glacier ice in mixture with MYI and FYI. In these cases the focus has been on the MYI and FYI as there can only be labeled two ice types in one polygon. This is for simplifying the training data for the machine learning algorithm. Separate iceberg surveys are provided for the 2 years, 2019 and 2020, in this study as icebergs are predominantly locked into the fast ice for the periods of the year when this is present.

Within each interpreted dataset there are four layer styles which provide the user with a quick interactive overview of the interpretations made and allows for editing. The four layer styles are: Fast ice (FA = 08), Dominant Stage of development (SA), Total Concentration (CT) and Ratio between Old ice and First-year ice.

4.1 April 2019

Filename:	Sea_Ice/seaice_alos2_20190427_134511.dbf Sea_Ice/seaice_alos2_20190427_134511.prj		Sea_Ice/seaice_alos2_20190427_134511.shp Sea_Ice/seaice_alos2_20190427_134511.shx
Satellite Data:			
Primary	alos2266062000-190427-wbdr1.5gpd.hhhv		
History/ Supplementary	CSKS_HH_20190416043206_20190416043224 S1A_EW_GRDM_1SDH_20190427T081002_20190427T081106_026973_030940_AA98		
Optical	S2B_MSIL1C_20190427T142749		S2A_MSIL1C_20190427T151911
Lidar	ICESat-2_ATL10_20190427		
Past Weather (48h)	Temperatures: -26 ℃ to -7 ℃. Alternating gentle breeze. No significant weather.		
Number of Polygons:	Water	Ice	**Total**
	13	162	**175**

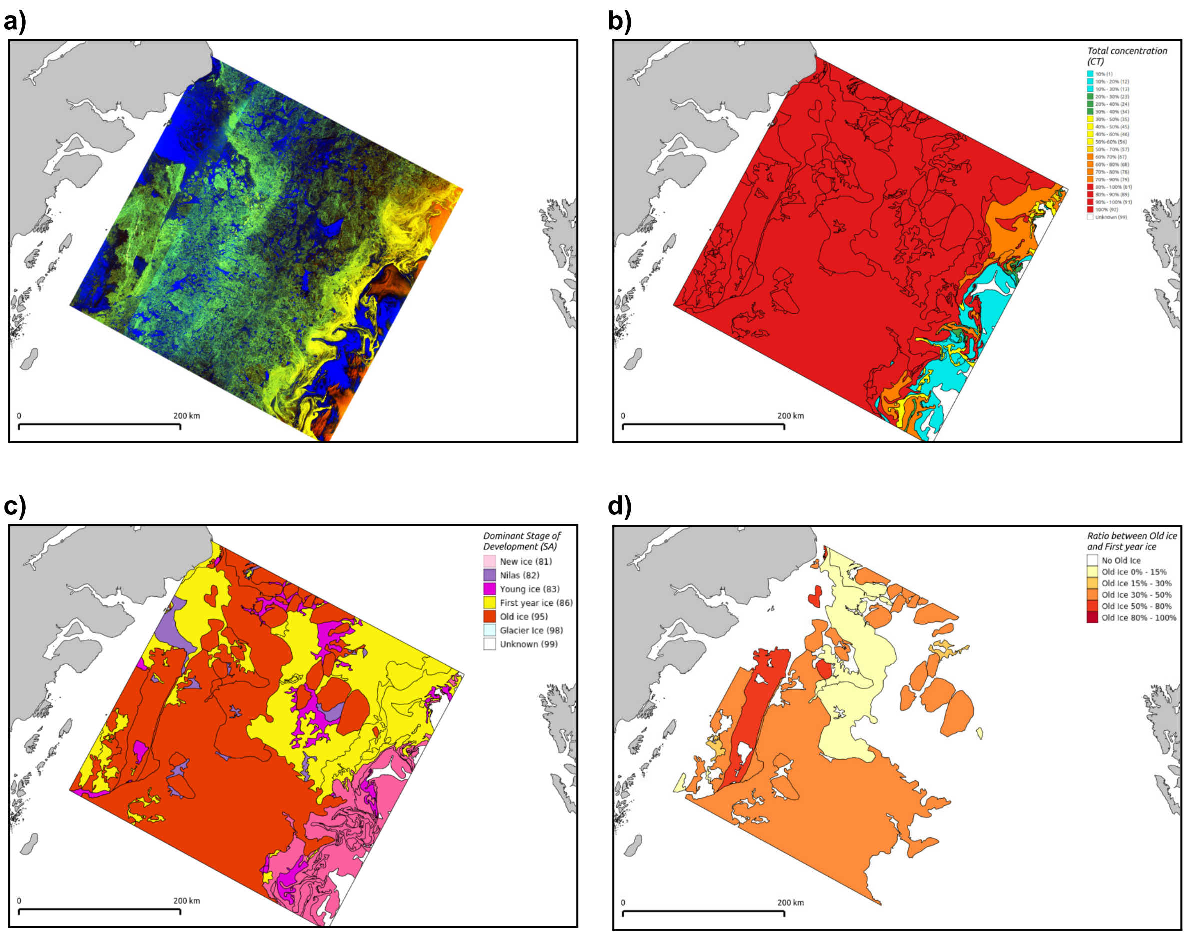

Figure 8: a) ALOS-2 quicklook for 27 April 2019. b) Interpreted total sea ice concentration (CT). c) Interpreted dominant stage of development (SA). d) Ratio between interpreted Old ice and FYI.

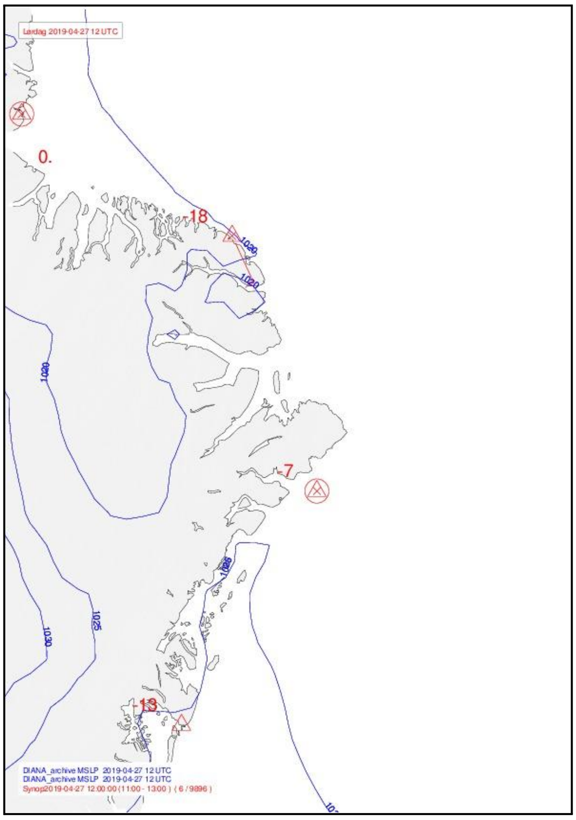

Figure 9: Prevailing air temperatures (°C), sea level pressure isobars (mbar) and winds (barbs) for 27 April 2019.

4.2 May 2019

Filename:	Sea_Ice/seaice_alos2_20190512_140602.dbf Sea_Ice/seaice_alos2_20190512_140602.prj	Sea_Ice/seaice_alos2_20190512_140602.shp Sea_Ice/seaice_alos2_20190512_140602.shx	
Satellite Data:			
Primary	alos2268282000-190512-wbdr1.5gpd.hhhv		
History/ Supplementary	CSKS_HH_20190520044411_20190520044430 S1B_EW_GRDM_1SDH_20190512T074427_20190512T074527_016208_01E80D_2A1A S1B_EW_GRDM_1SDH_20190512T074527_20190512T074627_016208_01E80D_5309 S1B_EW_GRDM_1SDH_20190512T092257_20190512T092336_016209_01E815_CEB5		
Optical	S2A_MSIL1C_20190513T153911	S2B_MSIL1C_20190512T165859	
Lidar	ICESat-2_ATL10_20190512		
Past Weather (48h)	Temperatures: -14 ℃ to -5 ℃. Alternating gentle breeze. Snow showers.		
Number of Polygons:	Water	Ice	**Total**
	0	71	**71**

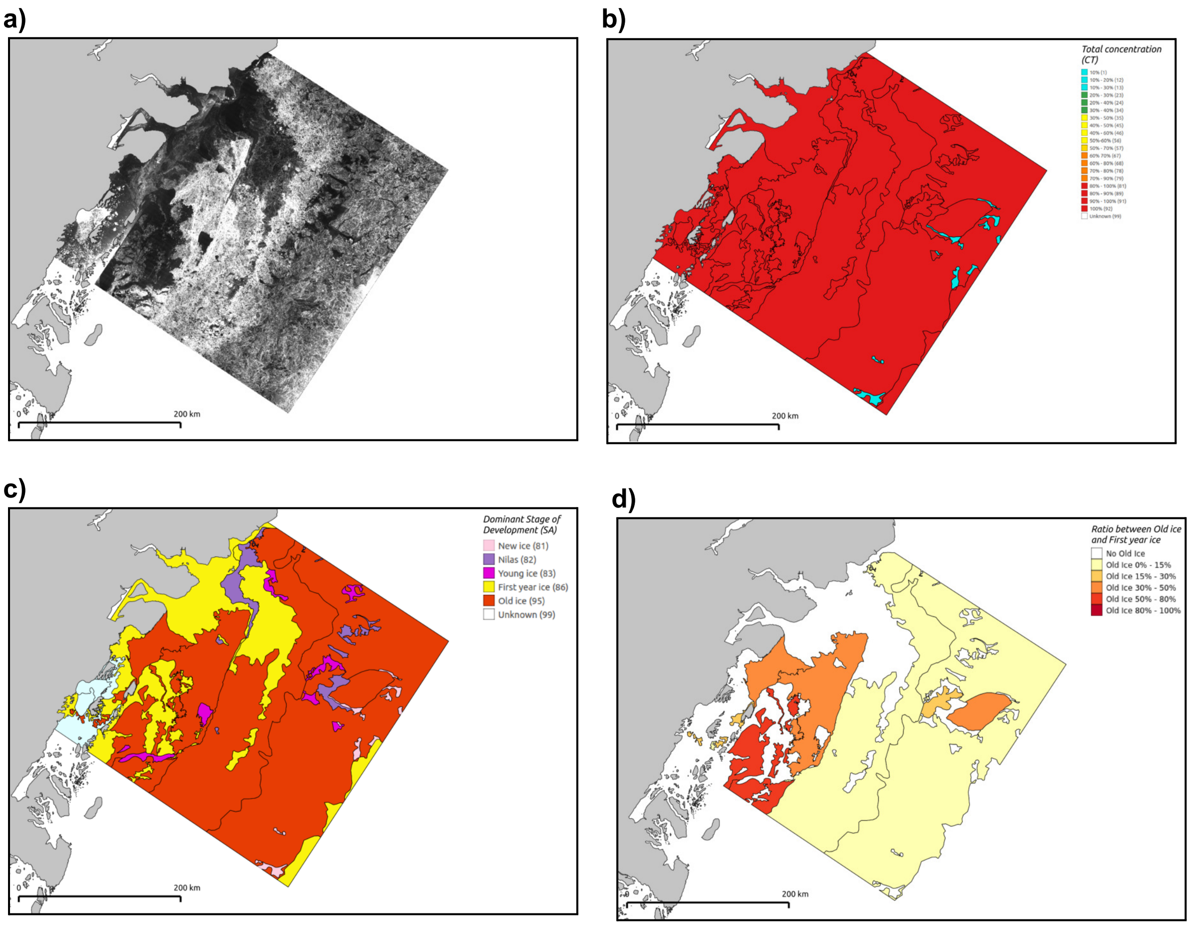

Figure 10: a) ALOS-2 quicklook for 12 May 2019. b) Interpreted total sea ice concentration (CT). c) Interpreted dominant stage of development (SA). d) Ratio between interpreted Old ice and FYI.

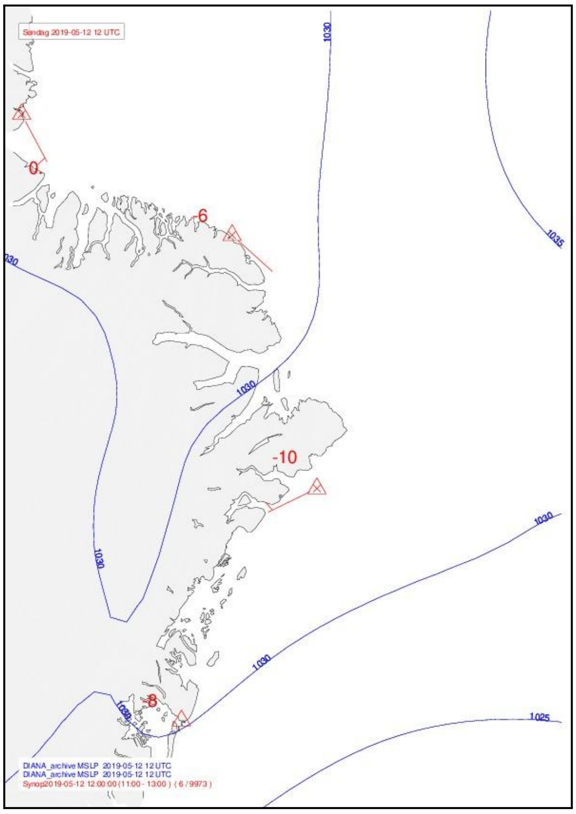

Figure 11: Prevailing air temperatures (°C), sea level pressure isobars (mbar) and winds (barbs) for 12 May 2019.

4.2.1 Icebergs

Filename:	Icebergs/icebergs_s2_2019.dbf Icebergs/icebergs_s2_2019.prj	Icebergs/icebergs_s2_2019.shp Icebergs/icebergs_s2_2019.shx
Satellite Data:		
Optical	S2B_MSIL1C_20190502T151809_N0207_R068_T28XDN_20190502T190011 S2B_MSIL1C_20190502T151809_N0207_R068_T28XDP_20190502T190011 S2B_MSIL1C_20190502T151809_N0207_R068_T28XDQ_20190502T190011 S2B_MSIL1C_20190502T151809_N0207_R068_T28XEN_20190502T190011 S2B_MSIL1C_20190502T151809_N0207_R068_T28XEP_20190502T190011 S2B_MSIL1C_20190502T151809_N0207_R068_T28XEQ_20190502T190011	
Number of Polygons:	**Total**	
	4,045	

Sentinel-2 data at 10 metres resolution was used to identify icebergs present in the region from 6 scenes from 2 May 2019.

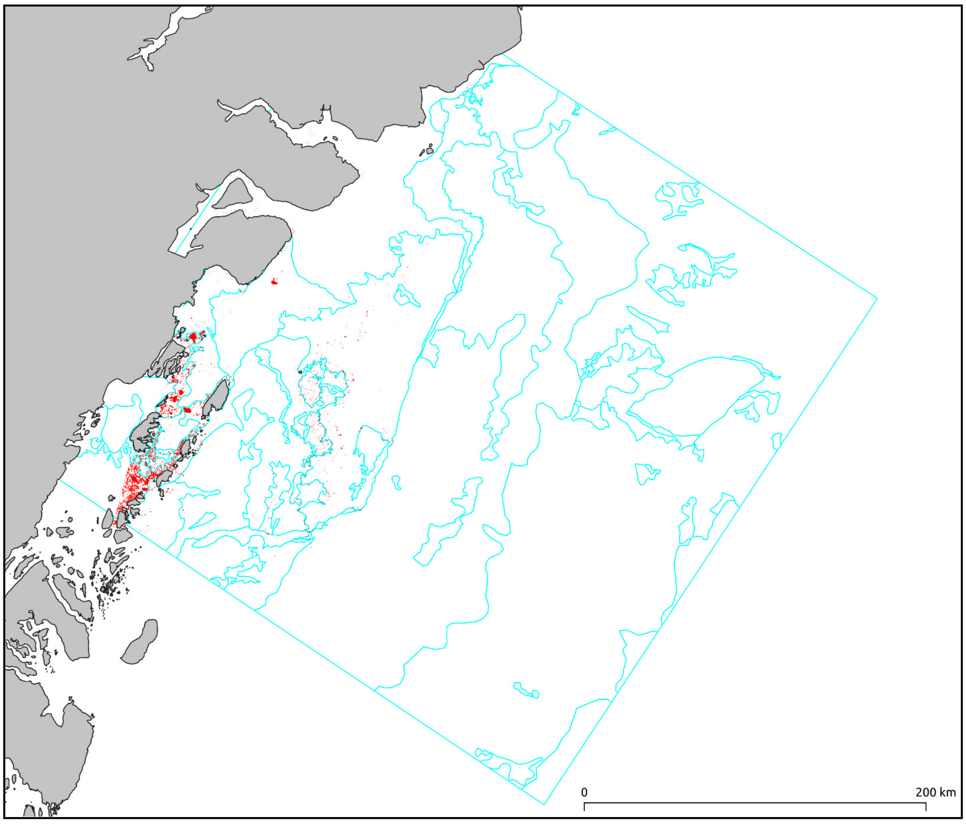

Figure 12: Icebergs in Belgica Bank region on 2 May 2019.

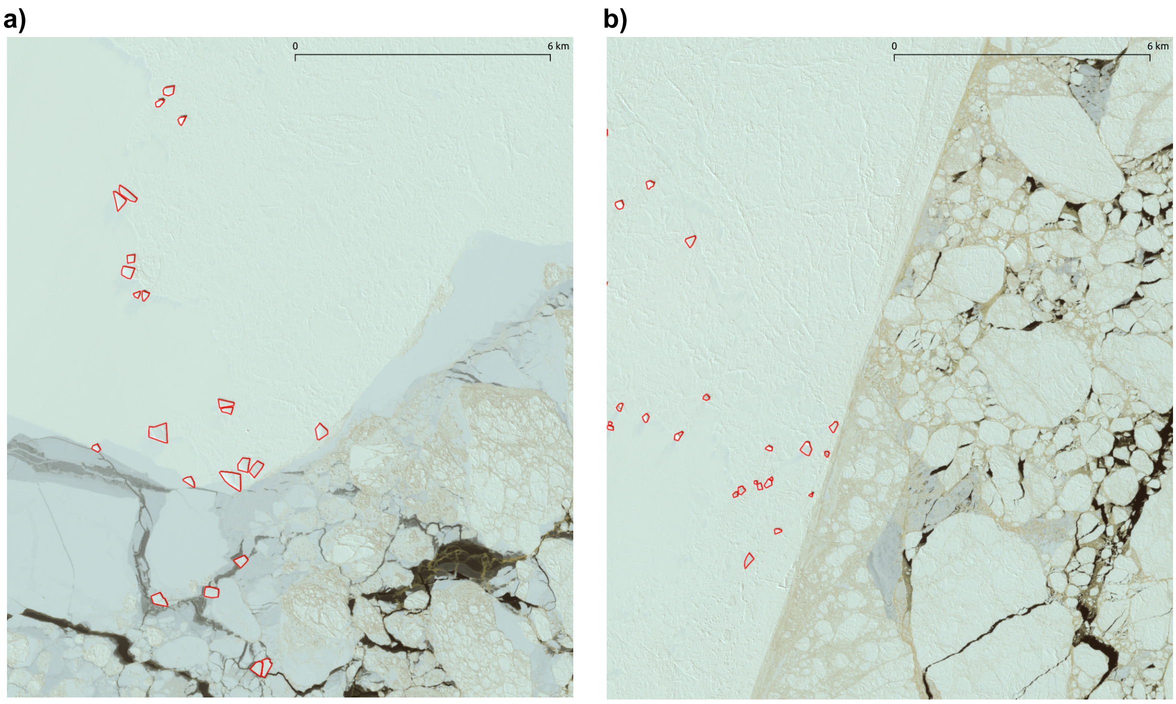

Figure 13: a) and b) examples of icebergs in S2B_MSIL1C_20190502T151809_N0207_R068_T28XEN_20190502T190011

4.3 June 2019

Filename:	Sea_Ice/seaice_alos2_20190622_134511.dbf Sea_Ice/seaice_alos2_20190622_134511.prj		Sea_Ice/seaice_alos2_20190622_134511.shp Sea_Ice/seaice_alos2_20190622_134511.shx
Satellite Data:			
Primary	alos2274342000-190622-wbdr1.5gpd.hhhv		
History/ Supplementary	CSKS_HH_20190616045014_20190616045033 S1B_EW_GRDM_1SDH_20190622T174012_20190622T174037_016812_01FA38_00A2 S1B_EW_GRDM_1SDH_20190622T173912_20190622T174012_016812_01FA38_DA6F S1A_EW_GRDM_1SDH_20190622T084259_20190622T084409_027790_032317_9CB1 S1B_EW_GRDM_1SDH_20190622T075247_20190622T075308_016806_01FA06_1444 S1A_EW_GRDM_1SDH_20190622T070417_20190622T070522_027789_03230C_C47B		
Optical	S2A_MSIL1C_20190621T160911 S2B_MSIL1C_20190621T151809		S2B_MSIL1C_20190621T165859
Lidar	ICESat-2_ATL10_20190622		
Past Weather (48h)	Temperatures: -2 ℃ to 3 ℃. Alternating slight breeze.Fog.		
Number of Polygons:	Water	Ice	**Total**
	0	82	**82**

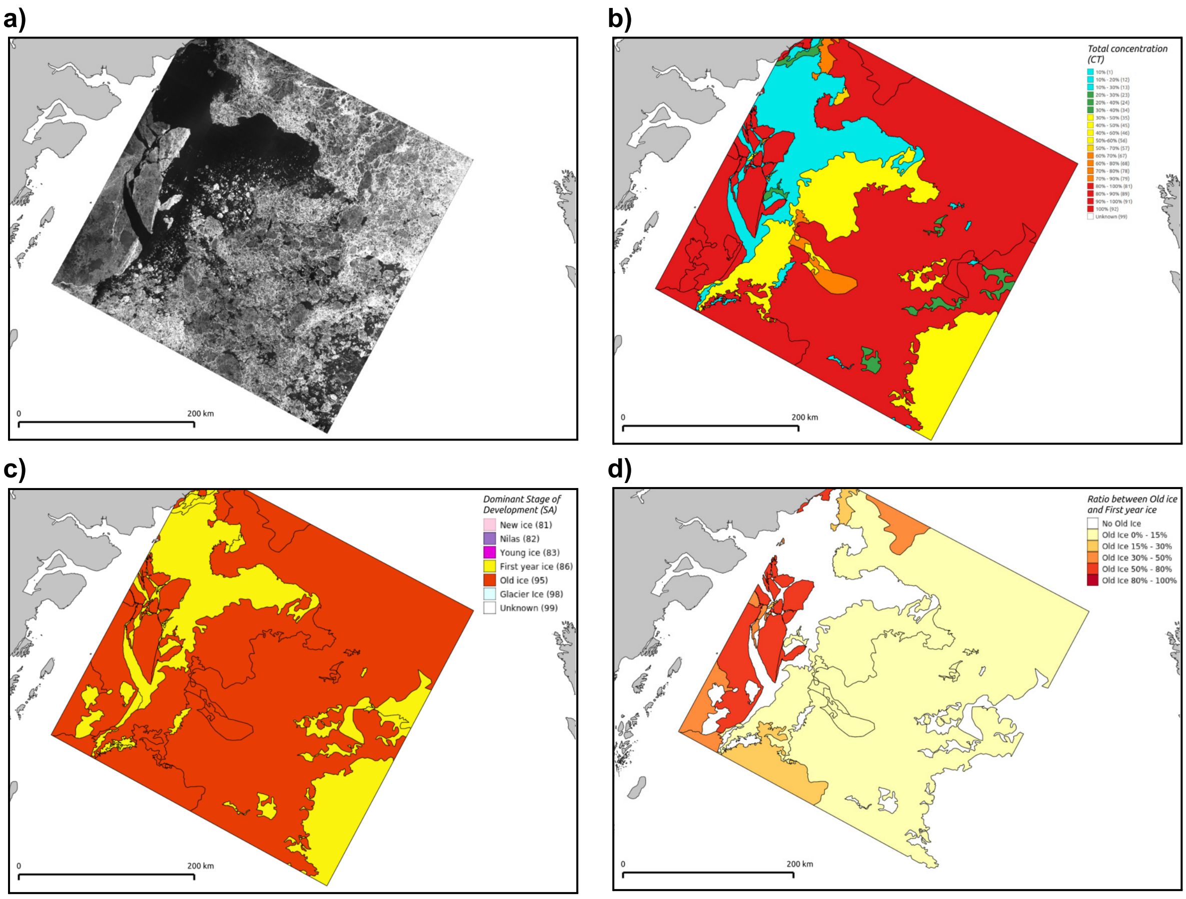

Figure 14: a) ALOS-2 quicklook for 22 June 2019. b) Interpreted total sea ice concentration (CT). c) Interpreted dominant stage of development (SA). d) Ratio between interpreted Old ice and FYI.

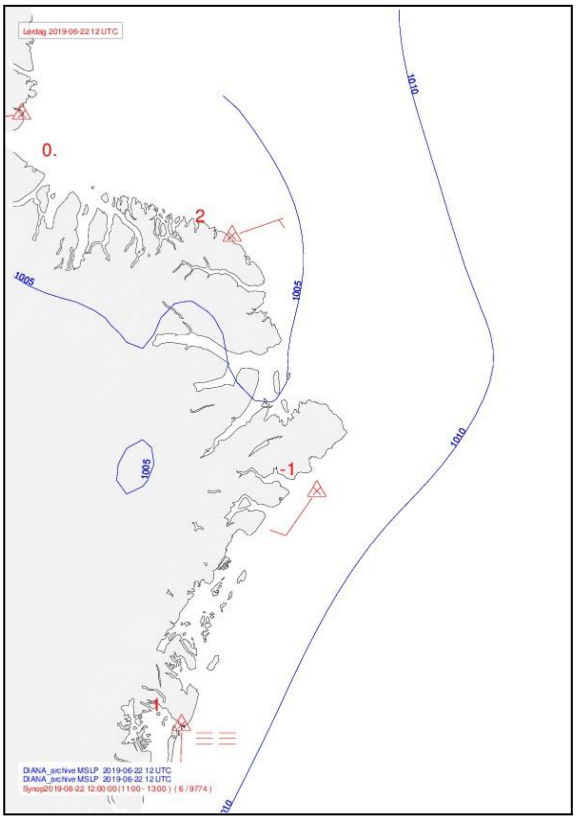

Figure 15: Prevailing air temperatures (°C), sea level pressure isobars (mbar) and winds (barbs) for 22 June 2019.

4.4 July 2019

Filename:	Sea_Ice/seaice_alos2_20190708_142655.dbf Sea_Ice/seaice_alos2_20190708_142655.prj	Sea_Ice/seaice_alos2_20190708_142655.shp Sea_Ice/seaice_alos2_20190708_142655.shx	
Satellite Data:			
Primary	alos2_2276712000_190708_wbdr1_5gpd_hhhv		
History/ Supplementary	CSKS_HH_20190729T045616_20190729T045635 S1A_EW_GRDM_1SDH_20190708T081005_20190708T081109_028023_032A2E_B30D S1A_EW_GRDM_1SDH_20190708T081109_20190708T081209_028023_032A2E_B61A		
Optical	S2A_MSIL1C_20190708T155911 S2B_MSIL1C_20190708T150809	S2A_MSIL1C_20190708T142001	
Lidar	None		
Past Weather (48h)	Temperatures: -2 ℃ to 6 ℃. Slight to gentle breeze from the south and west. Fog.		
Number of Polygons:	Water	Ice	**Total**
	0	78	**78**

a) b)
c) d)

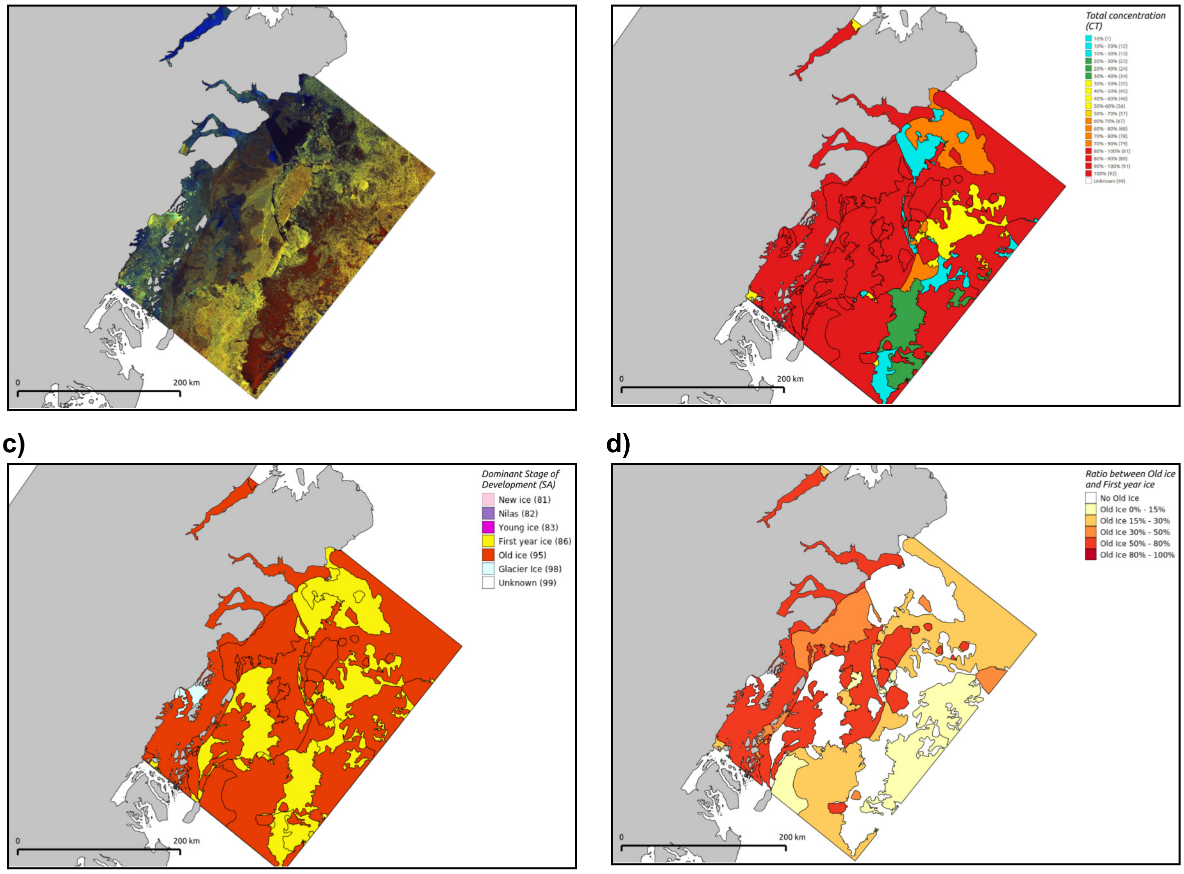

Figure 16: a) ALOS-2 quicklook for 8 July 2019. b) Interpreted total sea ice concentration (CT). c) Interpreted dominant stage of development (SA). d) Ratio between interpreted Old ice and FYI.

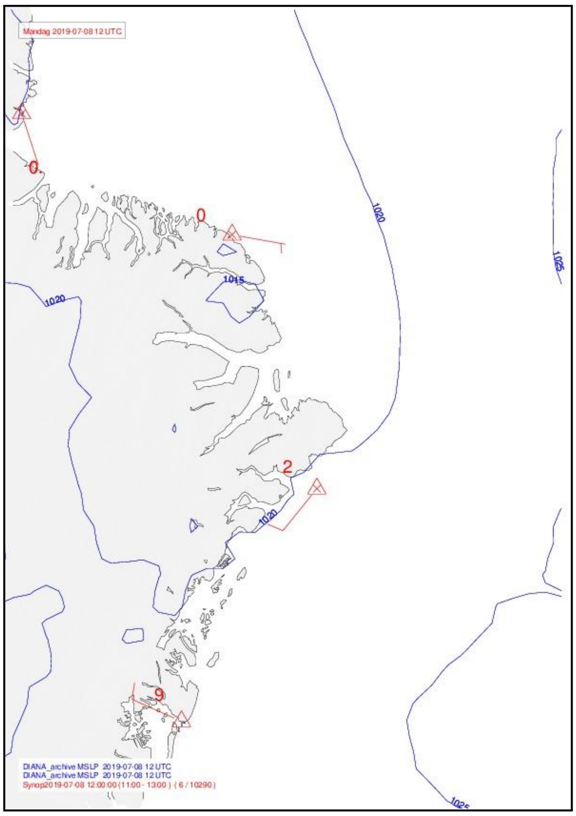

Figure 17: Prevailing air temperatures (°C), sea level pressure isobars (mbar) and winds (barbs) for 8 July 2019.

4.5 August 2019

Filename:	Sea_Ice/seaice_alos2_20190805_142655.dbf Sea_Ice/seaice_alos2_20190805_142655.shp Sea_Ice/seaice_alos2_20190805_142655.prj Sea_Ice/seaice_alos2_20190805_142655.shx		
Satellite Data:			
Primary	alos2_2280852000_190805_wbdr1_5gpd_hhhv		
History/ Supplementary	CSKS_HH_20190816T044415_20190816T044434 S1B_EW_GRDM_1SDH_20190805T082530_20190805T082630_017448_020D0D_2430 S1B_EW_GRDM_1SDH_20190805T082630_20190805T082730_017448_020D0D_B29D		
Optical	S2B_MSIL1C_20190805T142749 S2A_MSIL1C_20190805T151911		
Lidar	ICESat-2_ATL10_20190805		
Past Weather (48h)	Temperatures: -1 ℃ to 7 ℃. Alternating slight to gentle breeze. No significant weather.		
Number of Polygons:	Water	Ice	**Total**
	0	69	**69**

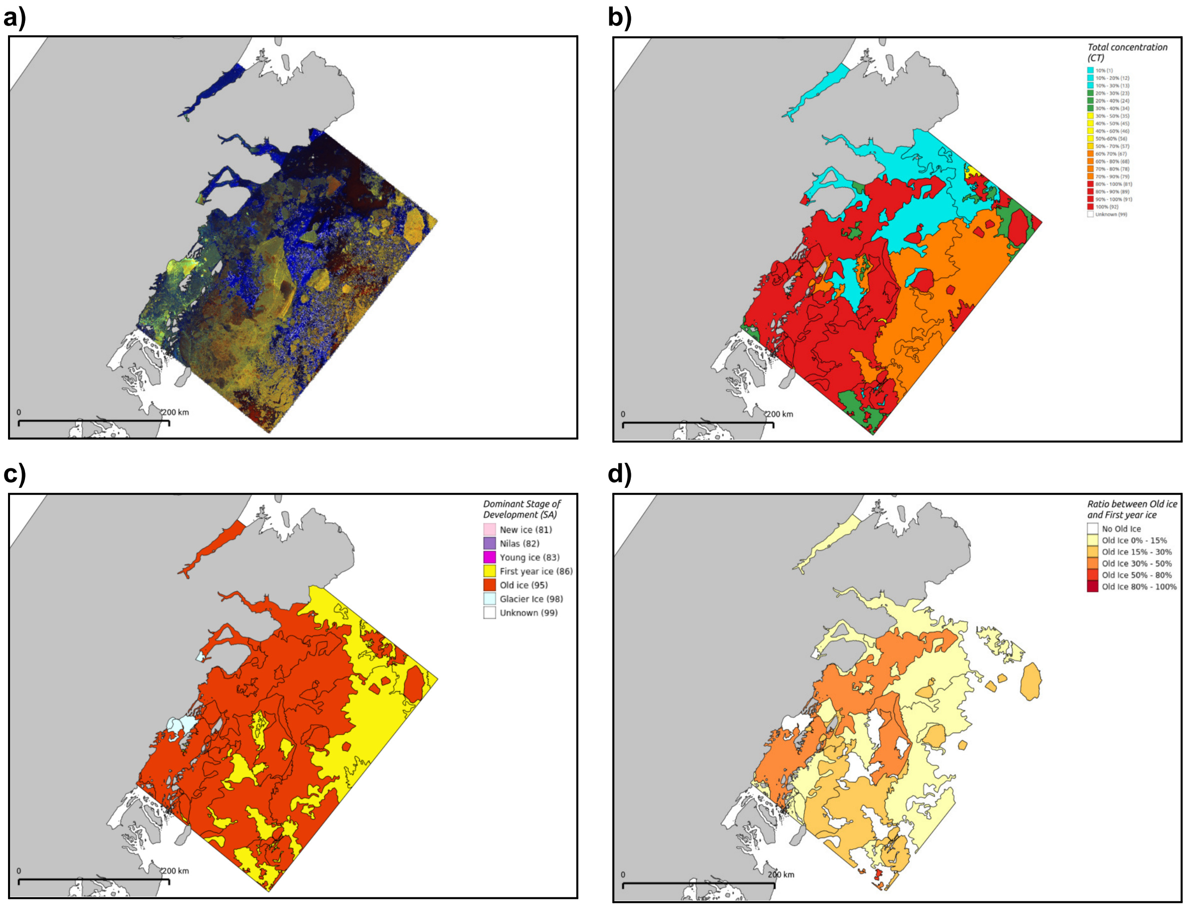

Figure 18: a) ALOS-2 quicklook for 5 August 2019. b) Interpreted total sea ice concentration (CT). c) Interpreted dominant stage of development (SA). d) Ratio between interpreted Old ice and FYI.

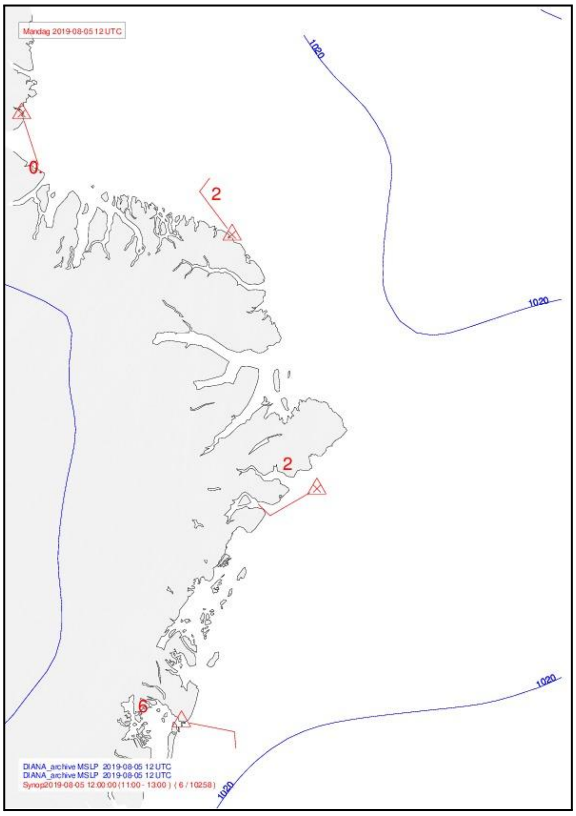

Figure 19: Prevailing air temperatures (°C), sea level pressure isobars (mbar) and winds (barbs) for 5 August 2019.

4.6 September 2019

Filename:	Sea_Ice/seaice_alos2_20190902_142655.dbf Sea_Ice/seaice_alos2_20190902_142655.prj		Sea_Ice/seaice_alos2_20190902_142655.shp Sea_Ice/seaice_alos2_20190902_142655.shx
Satellite Data:			
Primary	alos2_2284992000_190902_wbdr1_5gpd_hhhv		
History/ Supplementary	CSKS_HH_20190919T045020_20190919T045038 S1A_EW_GRDM_1SDH_20190902T084303_20190902T084408_028840_03449C_6414		
Optical	S2B_MSIL1C_20190902T170849 S2B_MSIL1C_20190902T152809		S2A_MSIL1C_20190902T143921
Lidar	ICESat-2_ATL10_20190902		
Past Weather (48h)	Temperatures: -4 ℃ to 4 ℃. Alternating slight breeze. No significant weather.		
Number of Polygons:	Water	Ice	**Total**
	0	95	**95**

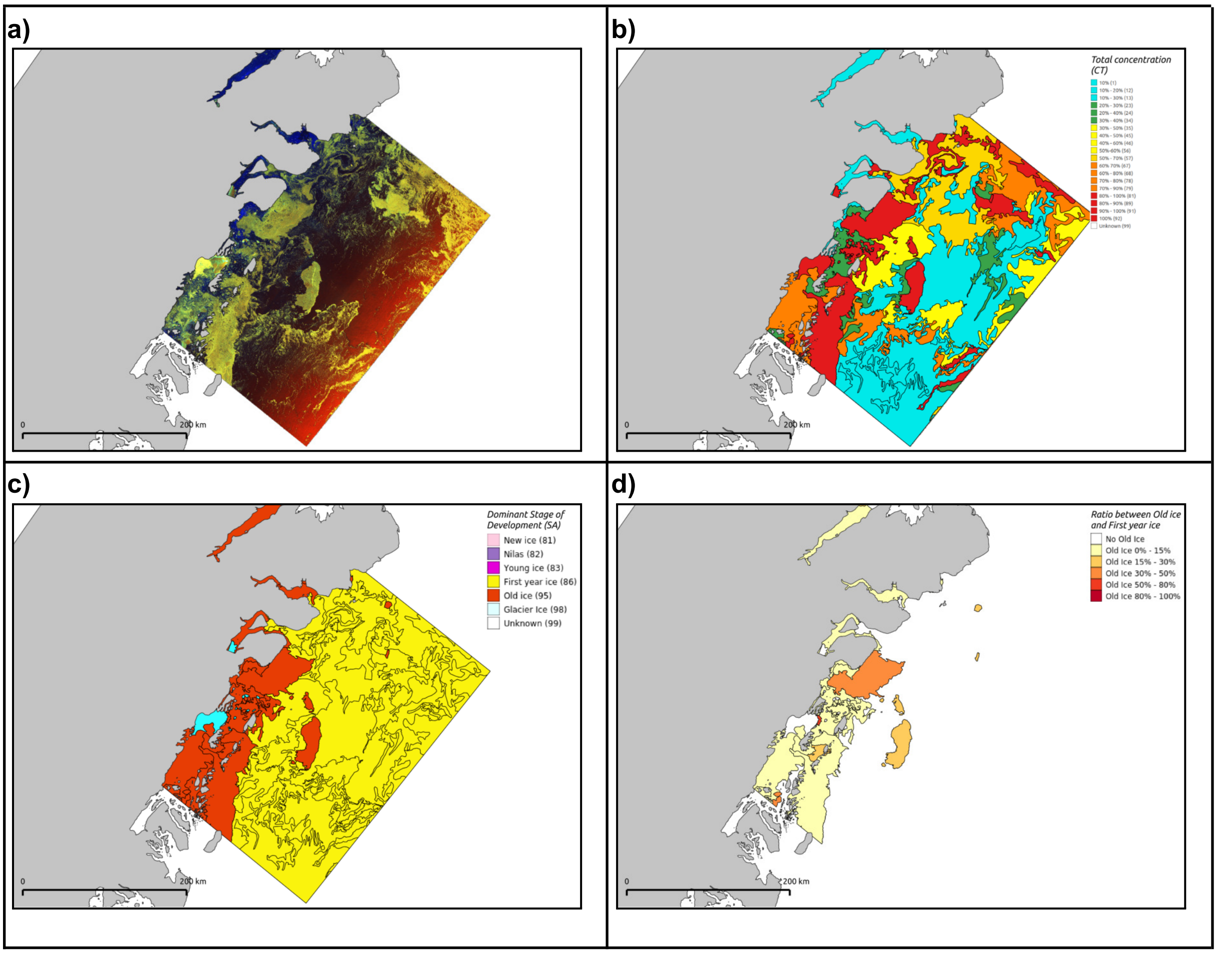

Figure 20: a) ALOS-2 quicklook for 2 September 2019. b) Interpreted total sea ice concentration (CT). c) Interpreted dominant stage of development (SA). d) Ratio between interpreted Old ice and FYI.

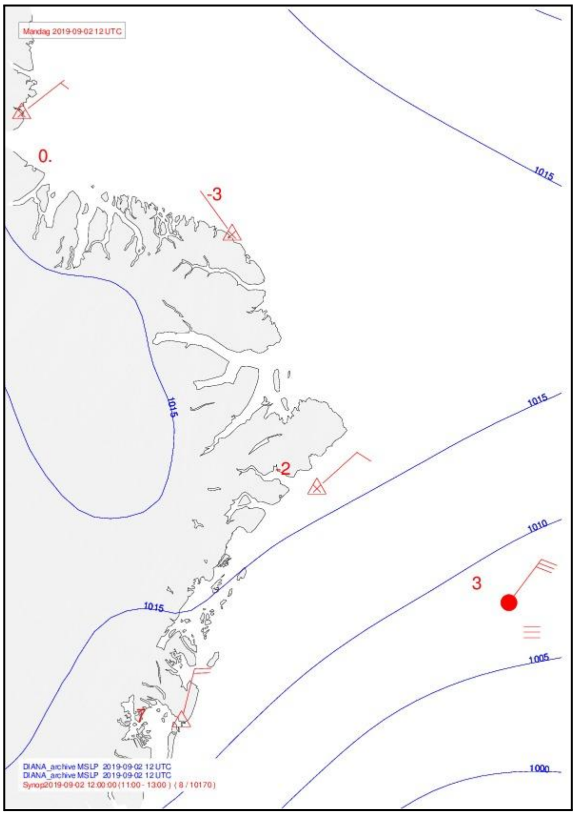

Figure 21: Prevailing air temperatures (°C), sea level pressure isobars (mbar) and winds (barbs) for 2 September 2019.

4.7 November 2019

Filename:	Sea_Ice/seaice_alos2_20191123_134513.dbf Sea_Ice/seaice_alos2_20191123_134513.prj	Sea_Ice/seaice_alos2_20191123_134513.shp Sea_Ice/seaice_alos2_20191123_134513.shx	
Satellite Data:			
Primary	alos2_2297112000_191123_wbdr1_5gpd_hhhv		
History/ Supplementary	CSKS_HH_20191120T044424_20191120T044443 S1B_EW_GRDM_1SDH_20191123T080909_20191123T081009_019052_023F44_875A S1B_EW_GRDM_1SDH_20191123T081009_20191123T081109_019052_023F44_EE89		
Optical	None		
Lidar	ICESat-2_ATL10_20191123		
Past Weather (48h)	Temperatures: -25 ℃ to -18 ℃. Slight breeze from the west. No significant weather.		
Number of Polygons:	Water	Ice	**Total**
	0	77	**77**

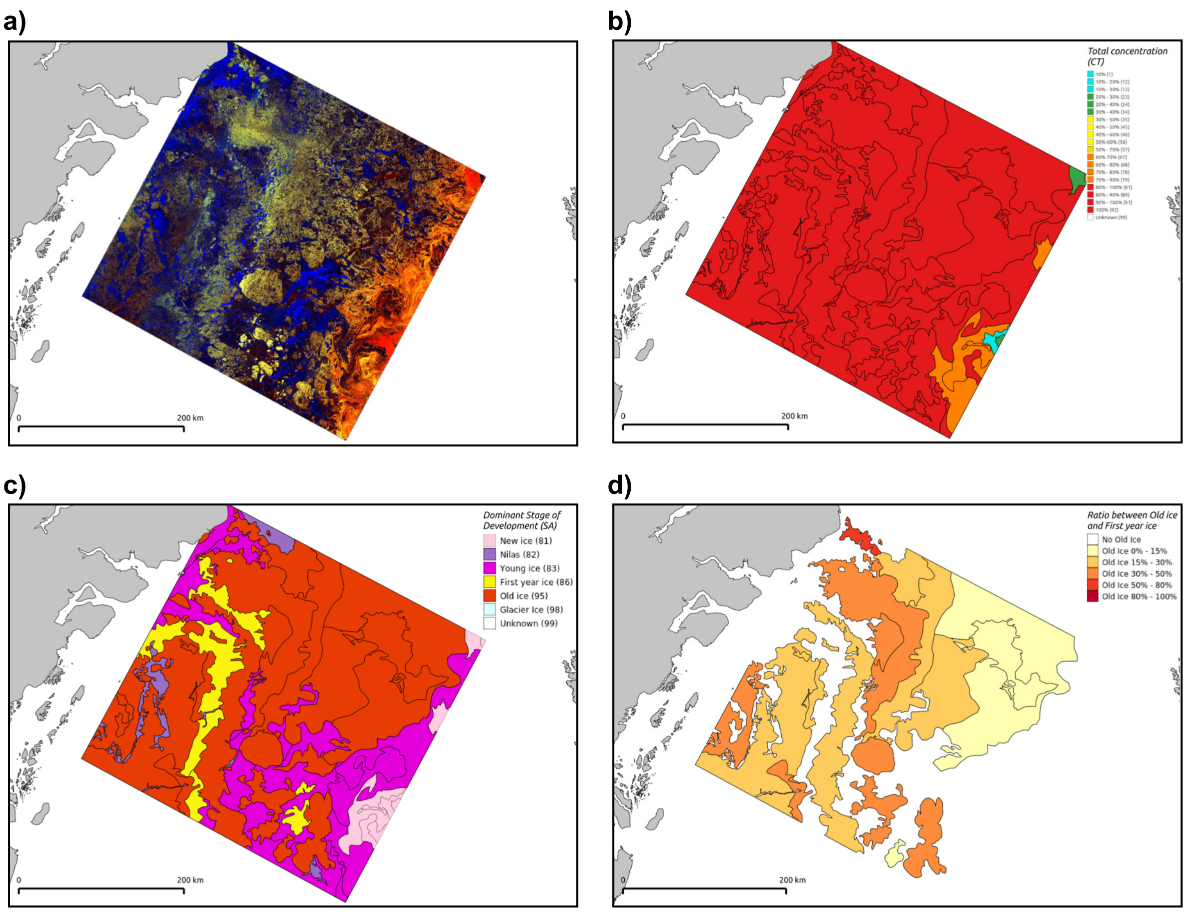

Figure 22: a) ALOS-2 quicklook for 23 November 2019. b) Interpreted total sea ice concentration (CT). c) Interpreted dominant stage of development (SA). d) Ratio between interpreted Old ice and FYI.

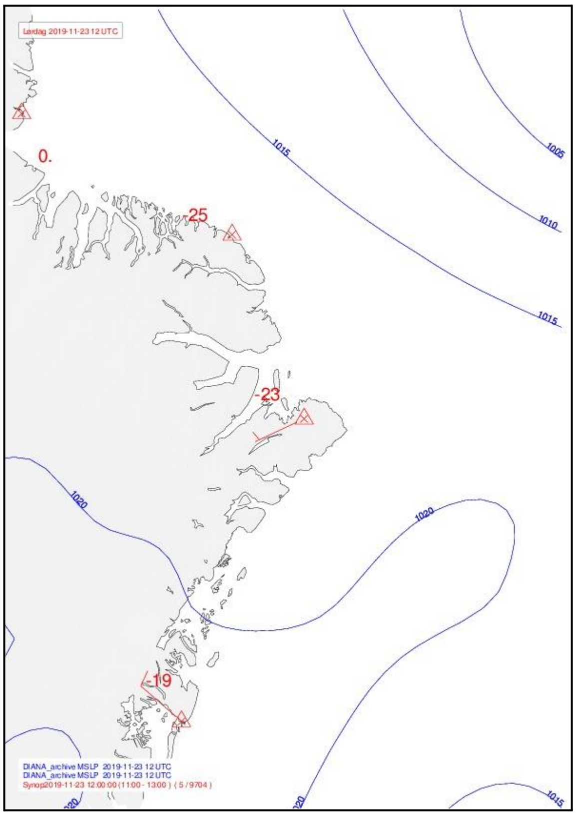

Figure 23: Prevailing air temperatures (°C), sea level pressure isobars (mbar) and winds (barbs) for 23 November 2019.

4.8 December 2019

Filename:	Sea_Ice/seaice_alos2_20191209_142658.dbf Sea_Ice/seaice_alos2_20191209_142658.prj	Sea_Ice/seaice_alos2_20191209_142658.shp Sea_Ice/seaice_alos2_20191209_142658.shx	
	Satellite Data:		
Primary	alos2_2299482000_191209_wbdr1_5gpd_hhhv		
History/ Supplementary	S1A_EW_GRDM_1SDH_20191209T082610_20191209T082715_030269_037604_9C97 S1A_EW_GRDM_1SDH_20191209T082715_20191209T082815_030269_037604_B370 S1A_EW_GRDM_1SDH_20191209T181252_20191209T181352_030275_037639_91E2 S1A_EW_GRDM_1SDH_20191209T181352_20191209T181501_030275_037639_3449		
Optical	None		
Lidar	ICESat-2_ATL10_20191209		
Past Weather (48h)	Temperatures: -31 ℃ to -19 ℃. Gentle breeze from the north. Snow showers.		
Number of Polygons:	Water	Ice	**Total**
	0	61	**61**

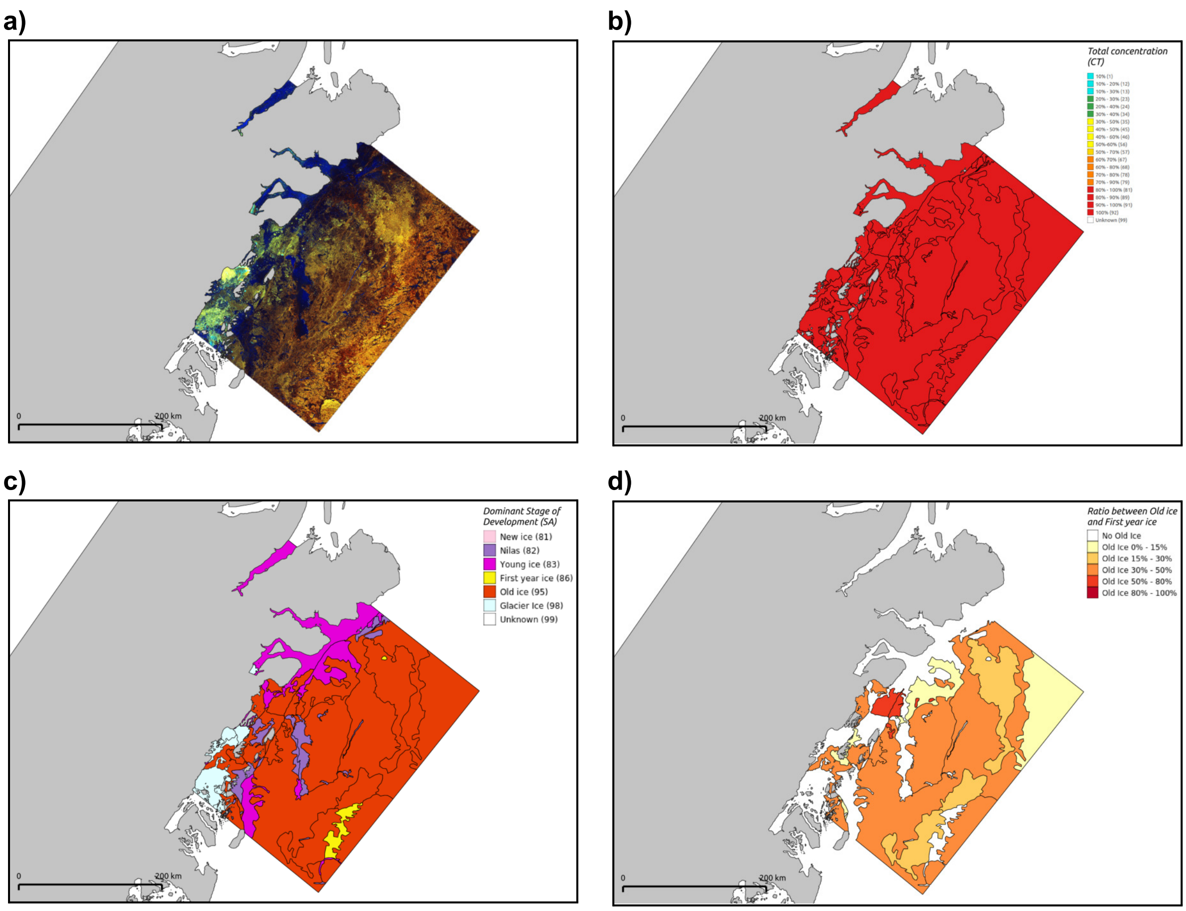

Figure 24: a) ALOS-2 quicklook for 9 December 2019. b) Interpreted total sea ice concentration (CT). c) Interpreted dominant stage of development (SA). d) Ratio between interpreted Old ice and FYI.

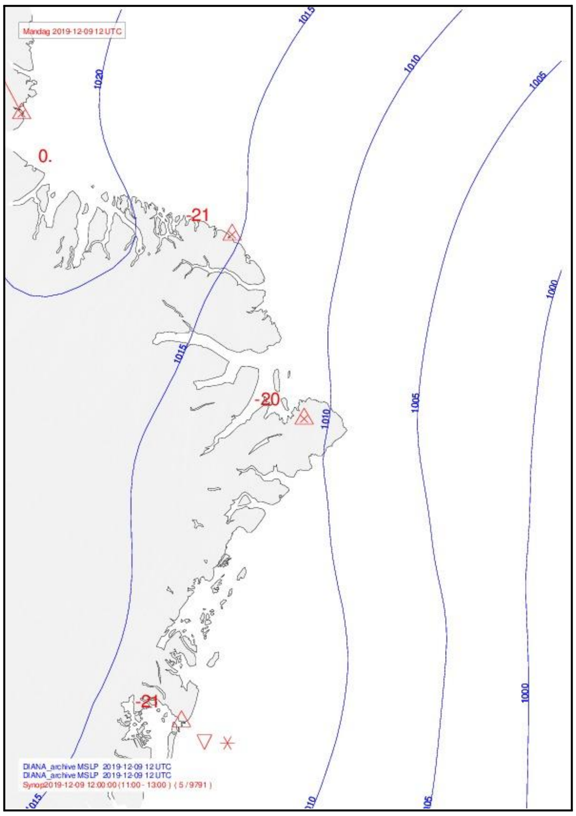

Figure 25: Prevailing air temperatures (°C), sea level pressure isobars (mbar) and winds (barbs) for 9 December 2019.

4.9 January 2020

Filename:	Sea_Ice/seaice_alos2_20200118_134515.dbf Sea_Ice/seaice_alos2_20200118_134515.prj	Sea_Ice/seaice_alos2_20200118_134515-shp Sea_Ice/seaice_alos2_20200118_134515.shx	
	Satellite Data:		
Primary	alos2_2305392000_200118_wbdr1_5gpd_hhhv		
History/ Supplementary	CSKS_HH_20200118T045025_20200118T045044 S1A_EW_GRDM_1SDH_20200118T075338_20200118T075443_030852_038A40_3265 S1B_EW_GRDM_1SDH_20200118T084150_20200118T084250_019869_02593F_F61E S1B_EW_GRDM_1SDH_20200118T084250_20200118T084350_019869_02593F_A6E3		
Optical	None		
Lidar	ICESat-2_ATL10_20200118		
Past Weather (48h)	Temperatures: -36 ℃ to -25 ℃. No wind data. Fog and snow showers.		
Number of Polygons:	Water	Ice	**Total**
	2	105	**107**

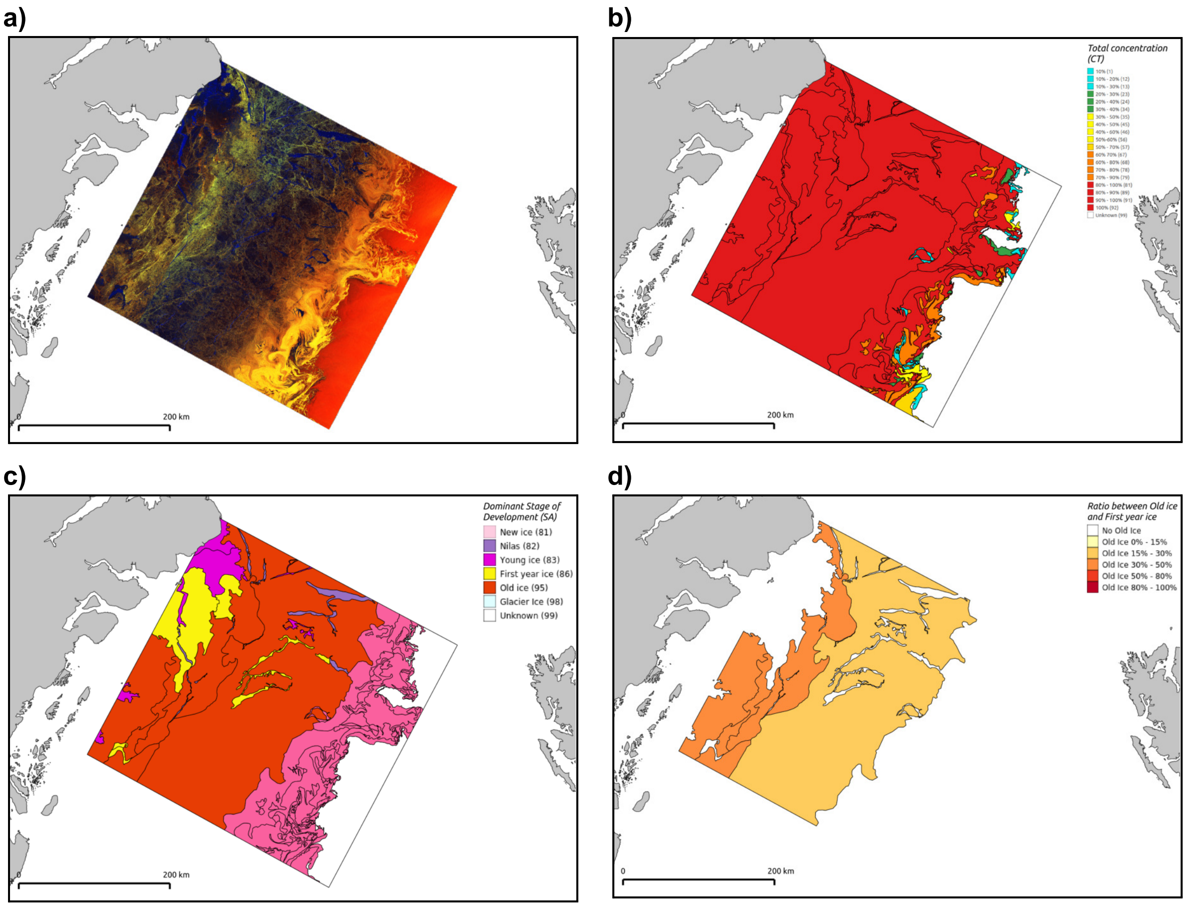

Figure 26: a) ALOS-2 quicklook for 18 January 2020. b) Interpreted total sea ice concentration (CT). c) Interpreted dominant stage of development (SA). d) Ratio between interpreted Old ice and FYI.

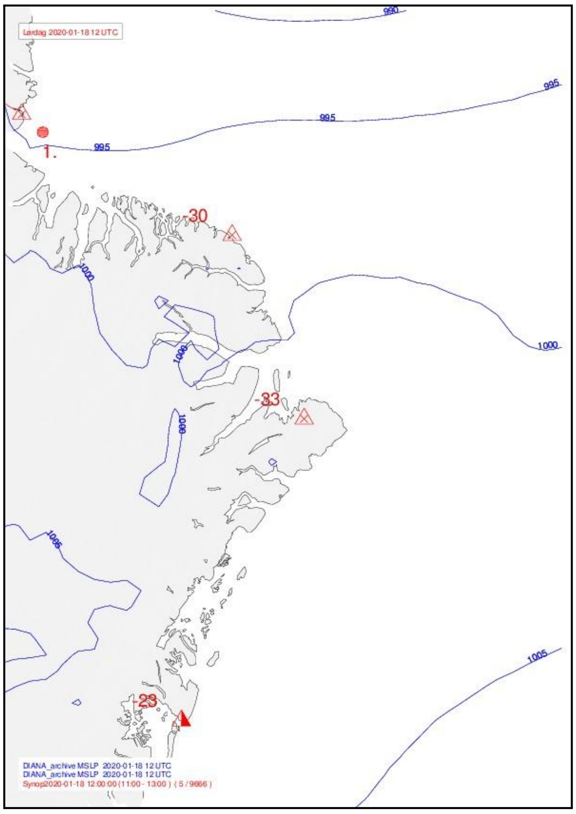

Figure 27: Prevailing air temperatures (°C), sea level pressure isobars (mbar) and winds (barbs) for 18 January 2020.

4.10 February 2020

Filename:	Sea_Ice/seaice_alos2_20200215_134515.dbf Sea_Ice/seaice_alos2_20200215_134515.prj	Sea_Ice/seaice_alos2_20200215_134515.shp Sea_Ice/seaice_alos2_20200215_134515.shx	
	Satellite Data:		
Primary	alos2_2309532000_200215_wbdr1_5gpd_hhhv		
History/ Supplementary	S1B_EW_GRDM_1SDH_20200215T080906_20200215T081006_020277_026664_EDF1 S1B_EW_GRDM_1SDH_20200215T081006_20200215T081106_020277_026664_5FD4		
Optical	None		
Lidar	ICESat-2_ATL10_20200215		
Past Weather (48h)	Temperatures: -34 ℃ to -24 ℃. Slight to gentle breeze from the west, northwest and southwest. Fog.		
Number of Polygons:	Water	Ice	**Total**
	3	83	**86**

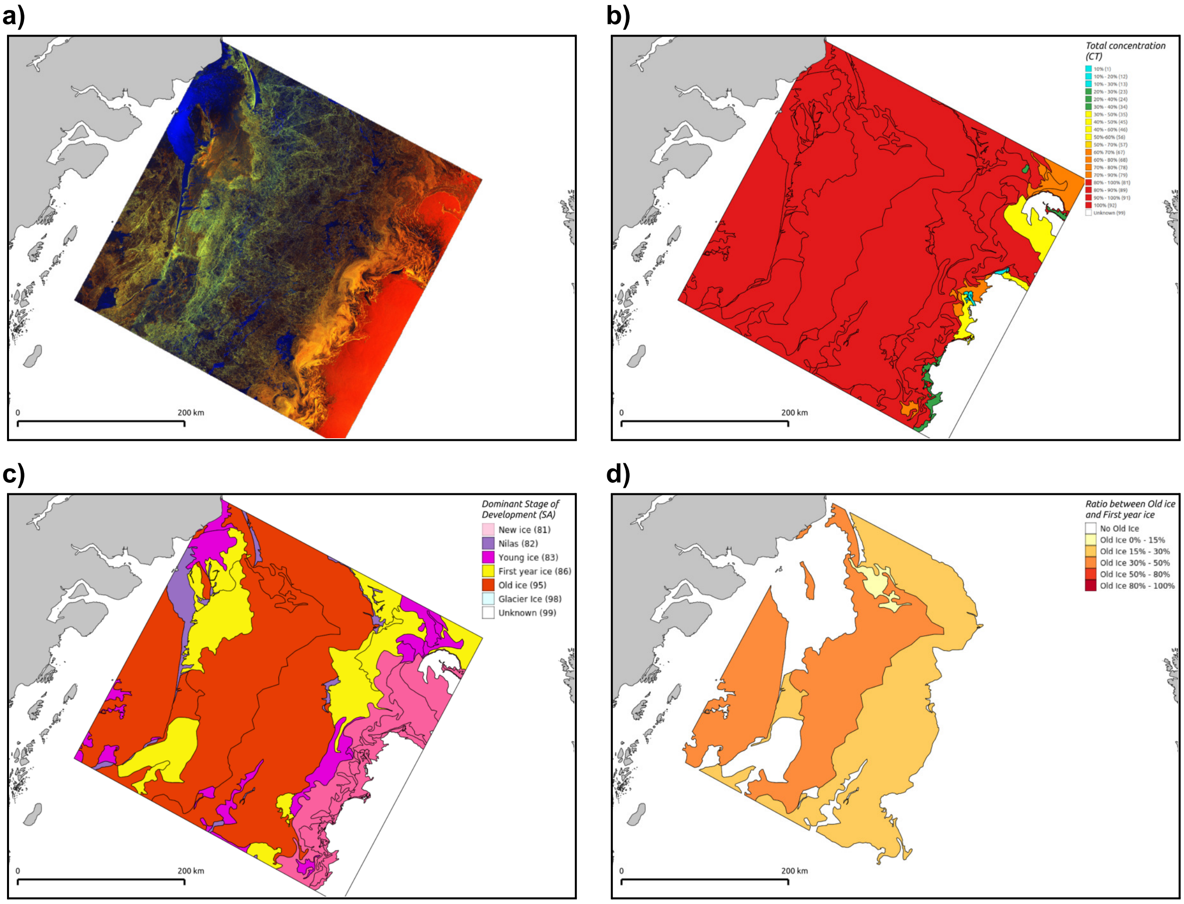

Figure 28: a) ALOS-2 quicklook for 15 February 2020. b) Interpreted total sea ice concentration (CT). c) Interpreted dominant stage of development (SA). d) Ratio between interpreted Old ice and FYI.

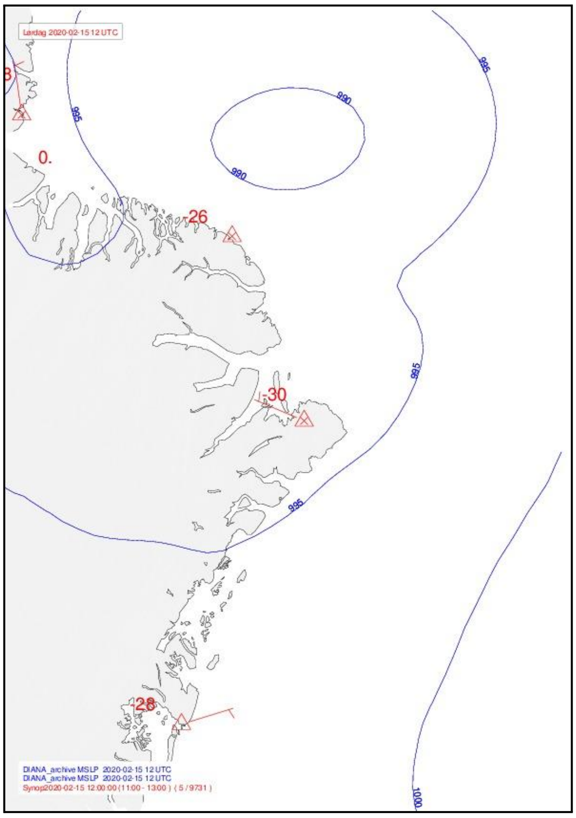

Figure 29: Prevailing air temperatures (°C), sea level pressure isobars (mbar) and winds (barbs) for 15 February 2020.

4.11 March 2020

Filename:	Sea_Ice/seaice_alos2_20200315_140606.dbf Sea_Ice/seaice_alos2_20200315_140606.shp Sea_Ice/seaice_alos2_20200315_140606.prj Sea_Ice/seaice_alos2_20200315_140606.shx		
Satellite Data:			
Primary	alos2_2313822000_200315_wbdr1_5gpd_hhhv		
History/ Supplementary	CSKS_HH_20200317T045626_20200317T045645 S1B_EW_GRDM_1SDH_20200315T081717_20200315T081817_020700_0273D2_5B76 S1B_EW_GRDM_1SDH_20200315T081817_20200315T081917_020700_0273D2_0EC9		
Optical	S2B_MSIL1C_20200316T154909 S2B_MSIL1C_20200316T140829		
Lidar	ICESat-2_ATL10_20200315		
Past Weather (48h)	Temperatures: -27 ℃ to -20 ℃. Strong breeze to fresh gale from the northwest. Snow showers and fog.		
Number of Polygons:	Water	Ice	**Total**
	0	62	**62**

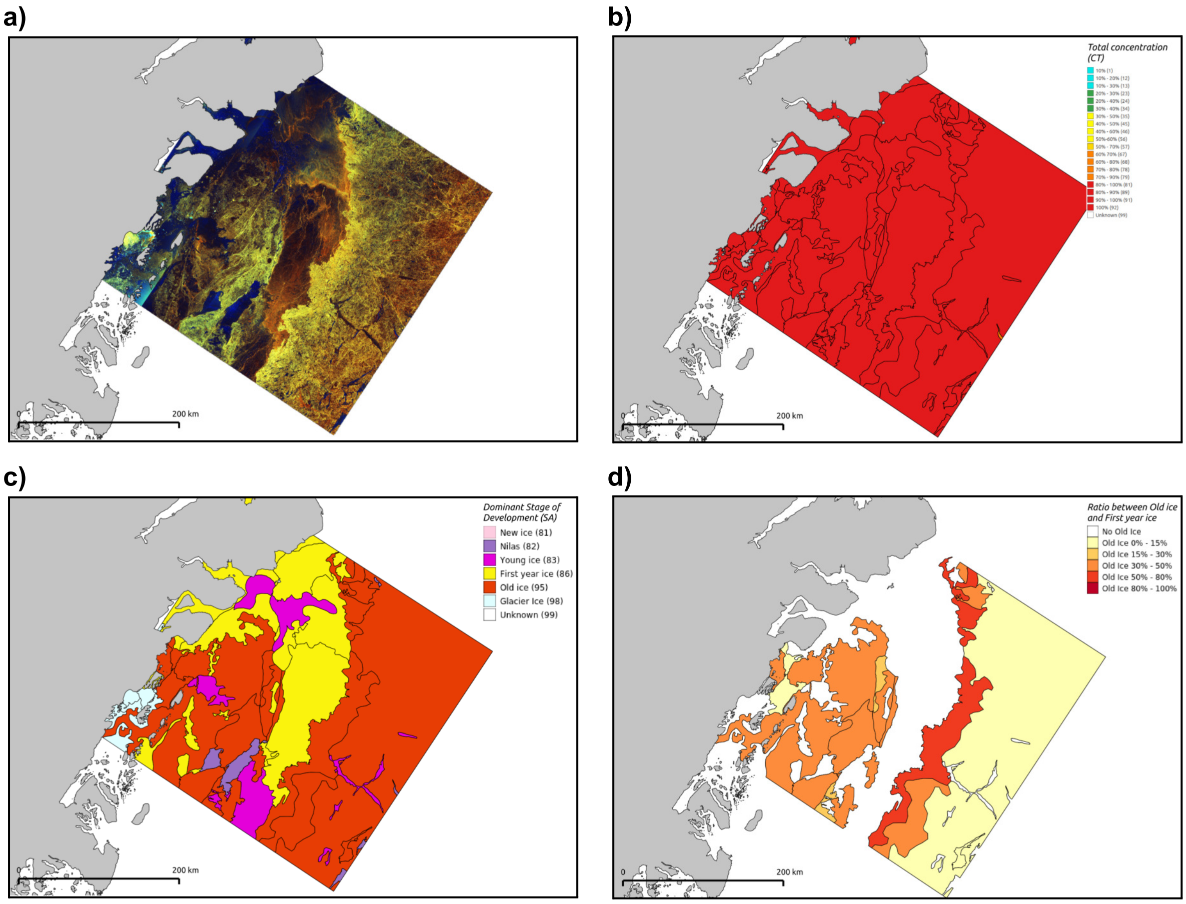

Figure 30: a) ALOS-2 quicklook for 15 March 2020. b) Interpreted total sea ice concentration (CT). c) Interpreted dominant stage of development (SA). d) Ratio between interpreted Old ice and FYI.

Meteorologisk institutt
Meteorological Institute
Org.no 971274042
post@met.no

Oslo
P.O. Box 43 Blindern
0313 Oslo, Norway
T. +47 22 96 30 00

Bergen
Allégaten 70
5007 Bergen, Norway
T. +47 55 23 66 00

Tromsø
P.O. Box 6314,
Langnes
9293 Tromsø, Norway
T. +47 77 62 13 00

www.met.no

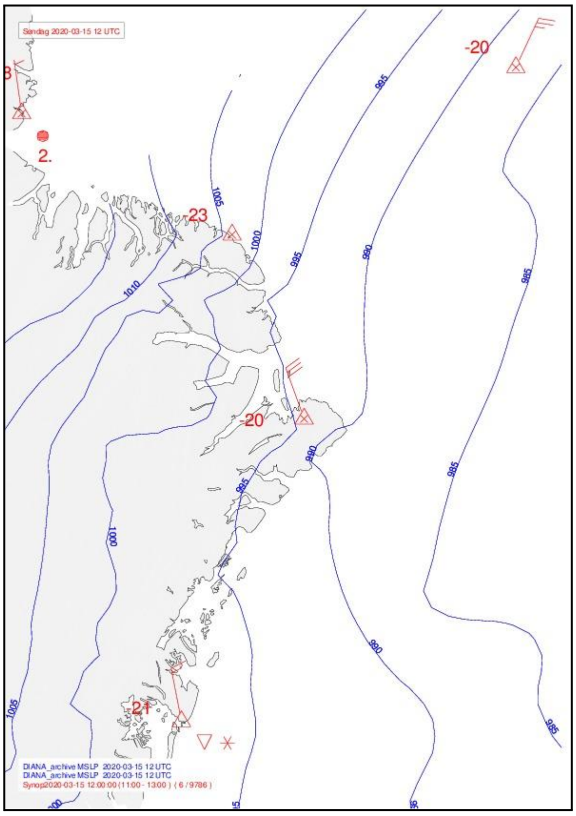

Figure 31: Prevailing air temperatures (°C), sea level pressure isobars (mbar) and winds (barbs) for 15 March 2020.

4.11.1 Icebergs

Filename:	Icebergs/icebergs_s2_2020.dbf Icebergs/icebergs_s2_2020.prj	Icebergs/icebergs_s2_2020.shp Icebergs/icebergs_s2_2020.shx
Satellite Data:		
Optical	S2A_MSIL1C_20200425T145921_N0209_R125_T28XDN_20200425T165958 S2A_MSIL1C_20200502T144921_N0209_R082_T28XDP_20200502T165213 S2A_MSIL1C_20200502T144921_N0209_R082_T28XDQ_20200502T165213 S2A_MSIL1C_20200502T144921_N0209_R082_T28XEN_20200502T165213 S2A_MSIL1C_20200502T144921_N0209_R082_T28XEP_20200502T165213 S2B_MSIL1C_20200502T153809_N0209_R011_T28XEQ_20200502T173254 S2B_MSIL1C_20200502T153809_N0209_R011_T29XNK_20200502T173254	
Number of Polygons:	**Total**	
	4,399	

As the region was only just coming out of the polar night in March, Sentinel-2 data at 10 metres resolution from 25 April and 2 May 2020 was used to identify icebergs present in the region and mostly embedded in the fast ice..

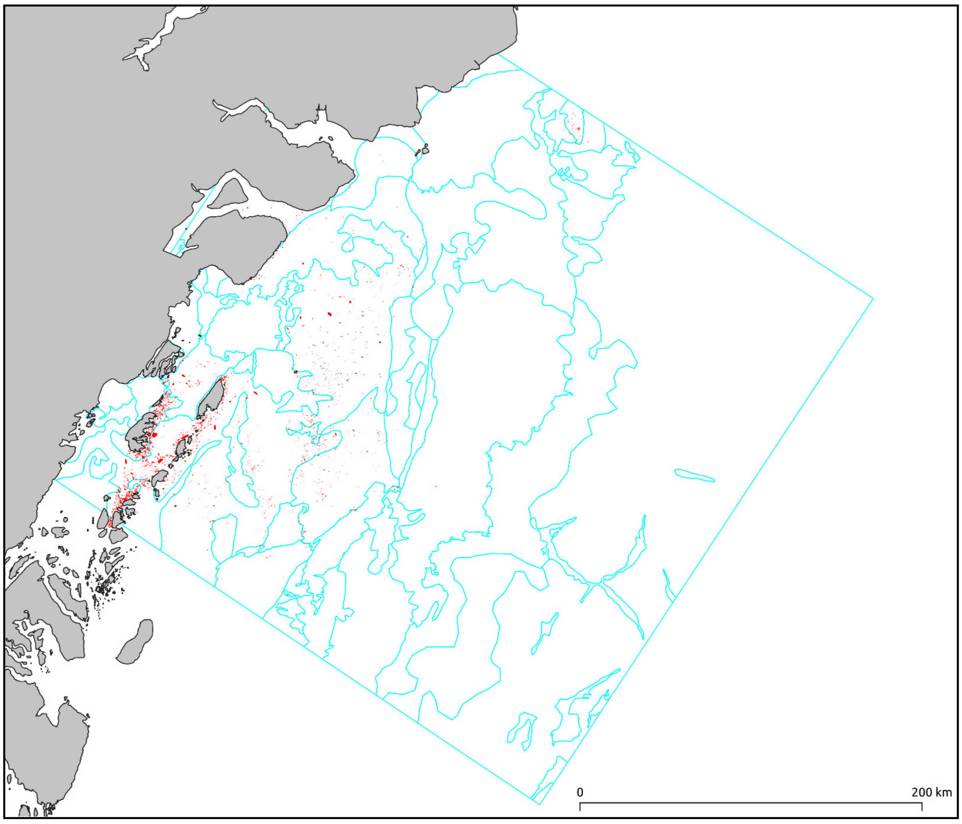

Figure 32: Icebergs in Belgica Bank region on 2 May 2020.

a) b)

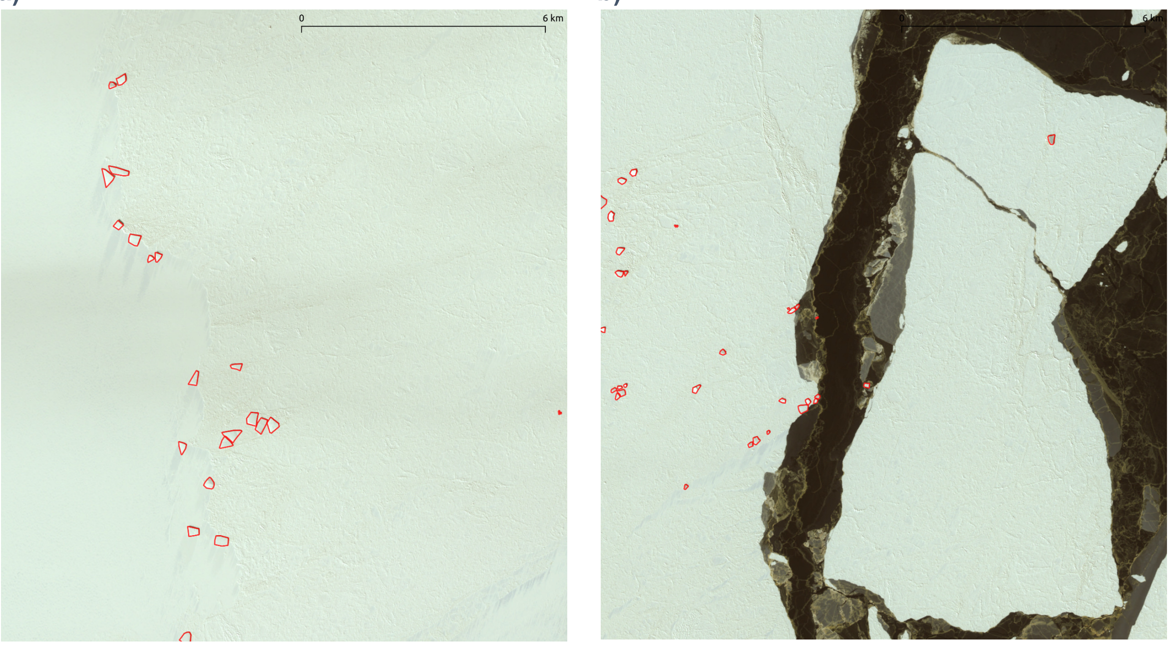

Figure 33: a) and b) examples of icebergs in
S2A_MSIL1C_20200502T144921_N0209_R082_T28XEN_20200502T165213
The geographical extents are the same as for May 2019 (Figure 13).

Meteorologisk institutt
Meteorological Institute
Org.no 971274042
post@met.no

Oslo
P.O. Box 43 Blindern
0313 Oslo, Norway
T. +47 22 96 30 00

Bergen
Allégaten 70
5007 Bergen, Norway
T. +47 55 23 66 00

Tromsø
P.O. Box 6314,
Langnes
9293 Tromsø, Norway
T. +47 77 62 13 00

www.met.no

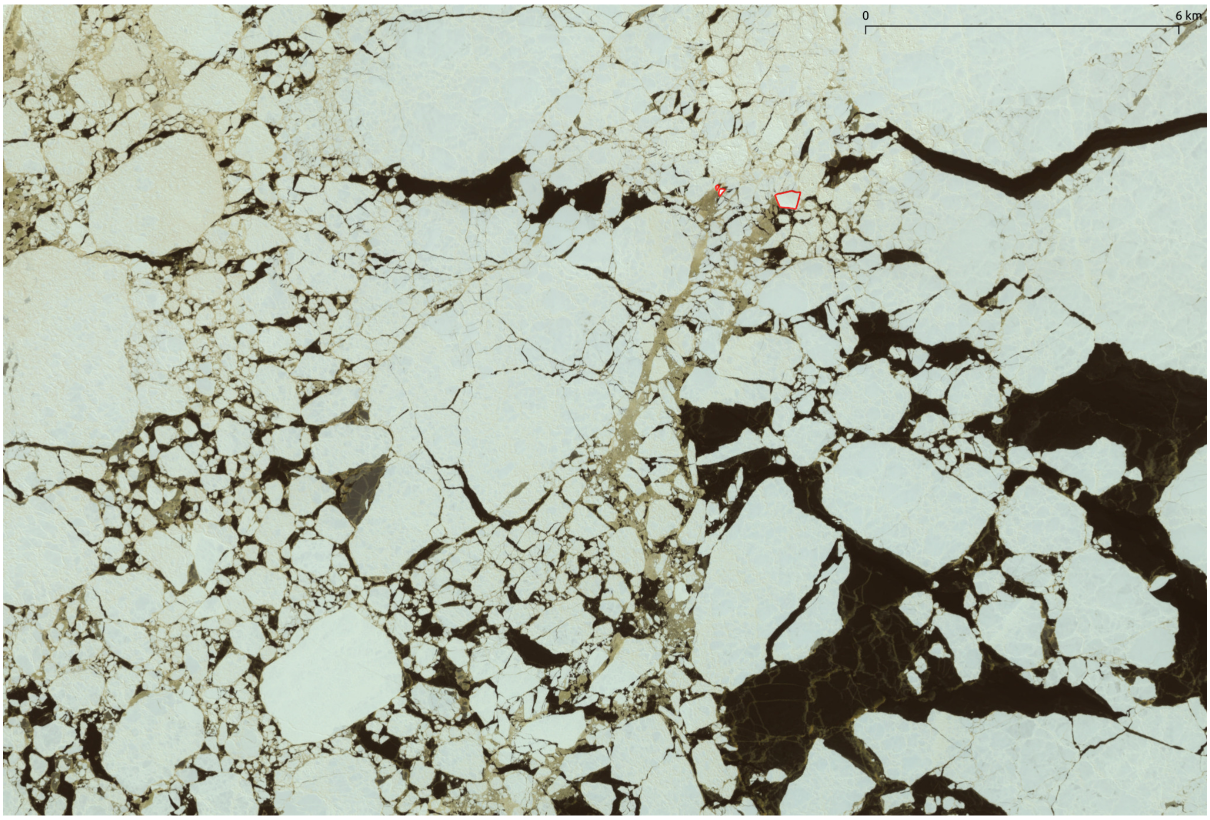

Figure 34: Iceberg tracks in sea ice in
S2A_MSIL1C_20200502T144921_N0209_R082_T28XEN_20200502T165213

5. Comparison ALOS-2 and Sentinel-1

12 example cases of comparing Sentinel-1 and ALOS-2 data throughout a year are presented in the following pages. The main objective was to compare Sentinel-1 and ALOS-2 images to detect synergies and examine anomalies in backscatter response with different sea ice situations and conditions.

COSMO-SkyMed, Sentinel-2 and ICESat-2 were also used here as supplementary data.

Meteorologisk institutt
Meteorological Institute
Org.no 971274042
post@met.no

Oslo
P.O. Box 43 Blindern
0313 Oslo, Norway
T. +47 22 96 30 00

Bergen
Allégaten 70
5007 Bergen, Norway
T. +47 55 23 66 00

Tromsø
P.O. Box 6314,
Langnes
9293 Tromsø, Norway
T. +47 77 62 13 00

www.met.no

5.1 Case 1: 2019-04-27 Thin Level Ice

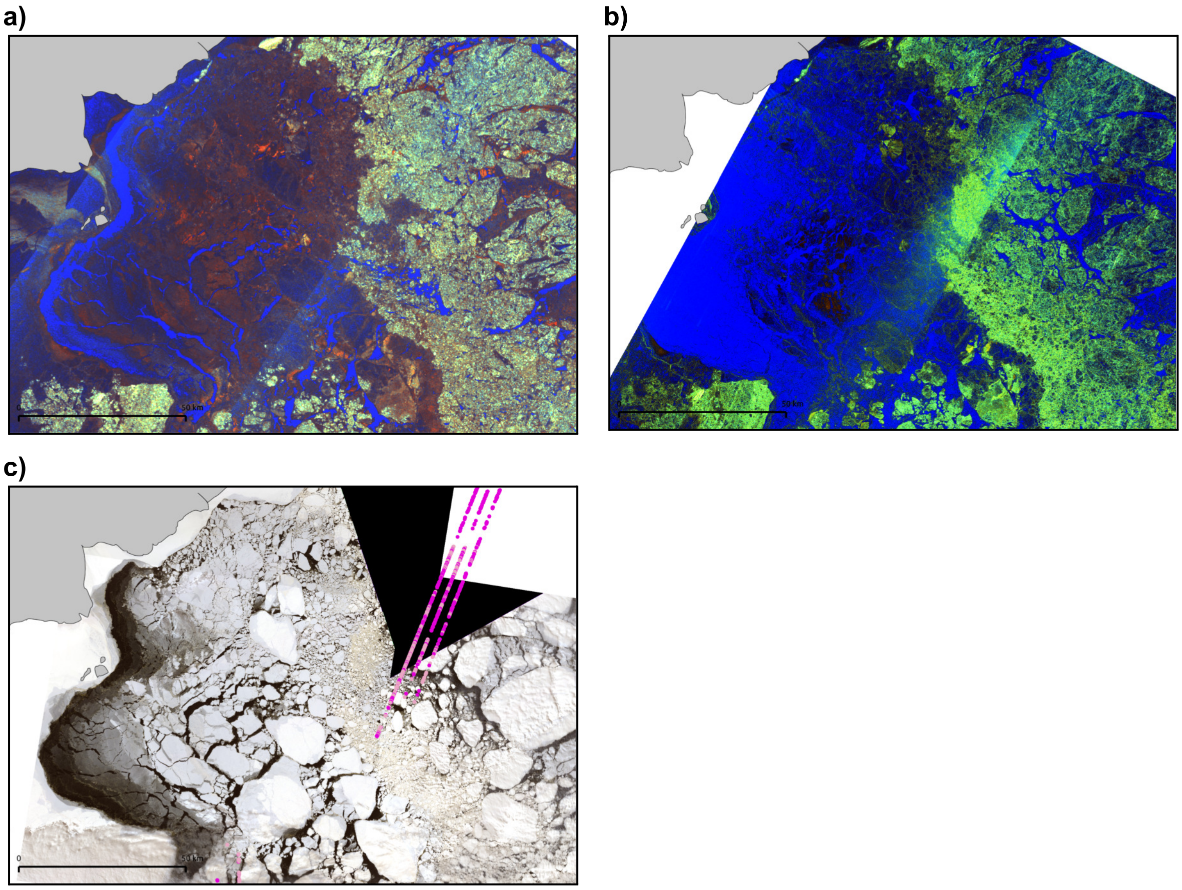

Figure 35: Case 1. a) Sentinel-1. b) ALOS-2. c) Sentinel-2 and ICESat-2. pink dots represent new ice, purple dots represent young ice.

When comparing S1 and ALOS-2 we can see that the thin ice which is near the fast ice boundary in the ALOS-2 image has a very uniform and low backscatter value, while the structure of the thin ice is more visible in the Sentinel-1 image (Figure 35). This makes it difficult to differentiate between new nilas ice and the level thin ice floes near the fast ice boundary with ALOS-2 compared to Sentinel-1 and Sentinel-2. This is likely due to the lower frequency of ALOS-2 (1.2 GHz) compared to Sentinel-1 (5.405 GHz).

5.2 Case 2: 2019-04-27 Old ice and FYI

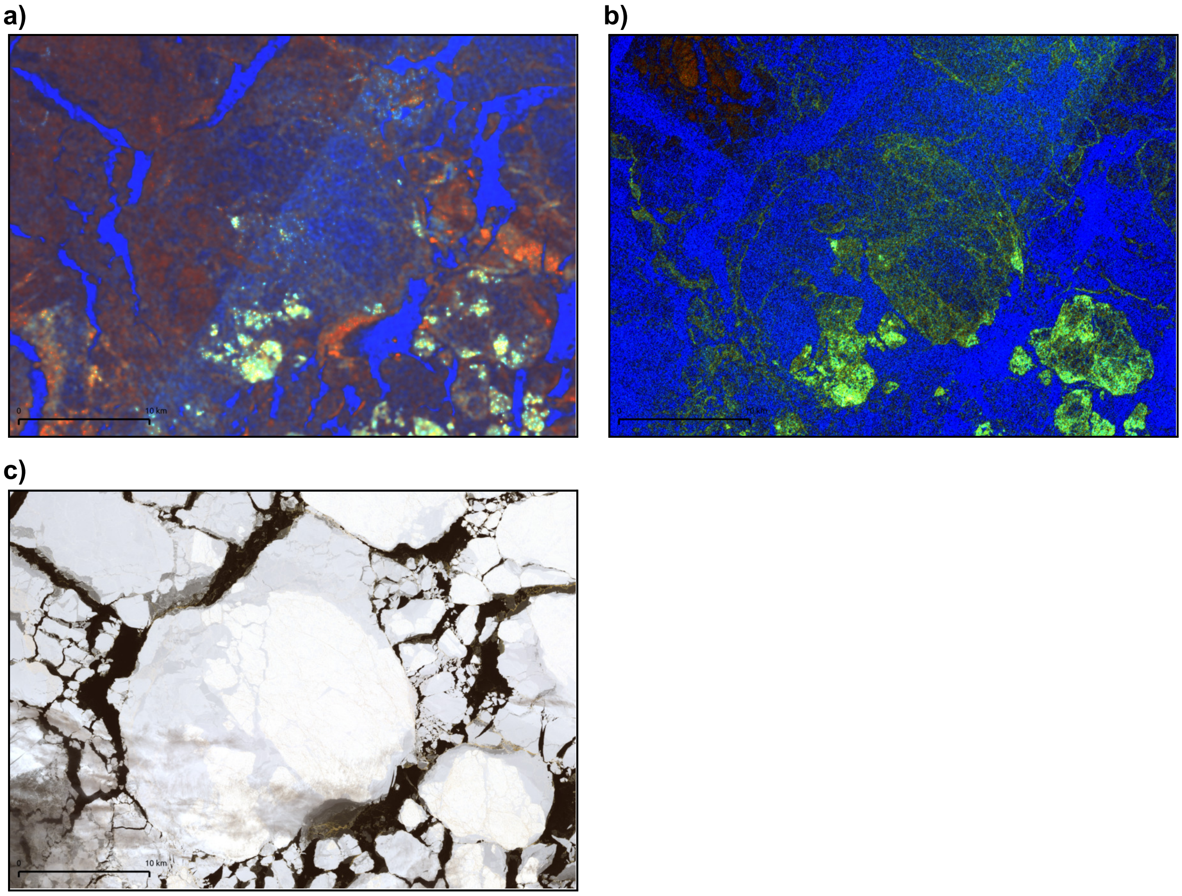

Figure 36: Case 2. a) Sentinel-1. b) ALOS-2. c) Sentinel-2.

The brighter parts of the giant floe is interpreted to represent multiyear ice which is encapsulated by first-year ice. Notice how the signature and structure of the MYI floes is more visible with the ALOS-2 image than the Sentinel-1 image (Figure 36).

Meteorologisk institutt
Meteorological Institute
Org.no 971274042
post@met.no

Oslo
P.O. Box 43 Blindern
0313 Oslo, Norway
T. +47 22 96 30 00

Bergen
Allégaten 70
5007 Bergen, Norway
T. +47 55 23 66 00

Tromsø
P.O. Box 6314,
Langnes
9293 Tromsø, Norway
T. +47 77 62 13 00

www.met.no

5.3 Case 3: 2019-04-27 Floes

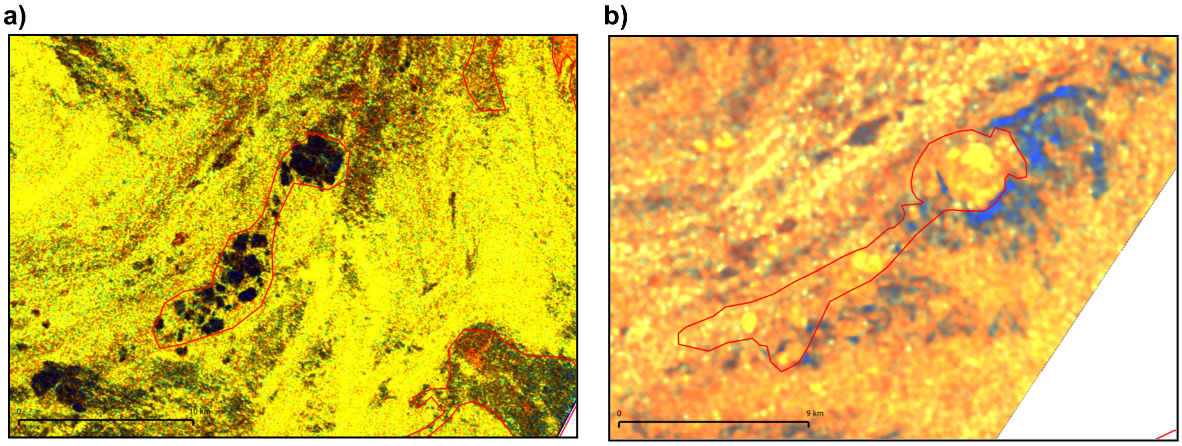

Figure 37: Case 3. a) ALOS-2 b) Sentinel-1.

The floes are easily identified in the ALOS-2 image, reflecting a much lower backscatter signature than its surroundings (Figure 37a). While examining presumably the same floes in the Sentinel-1 image they have a higher backscatter than its surroundings making it difficult to distinguish them in the surrounding high reflecting small floes (Figure 37b).

5.4 Case 4: 2019-05-12 Water and Nilas

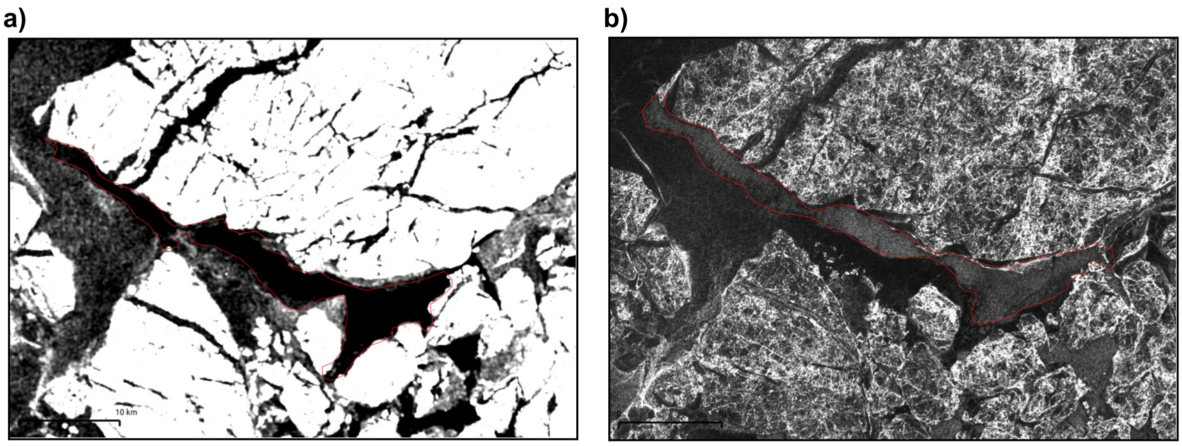

Figure 38: Case 4. a) Sentinel-1. b) ALOS-2.

The area within the red polygon is interpreted as water- This is best illustrated by the ALOS-2, where the backscatter is higher than the black area which is interpreted to be level ice (Figure 38). This might be due to the wind effect and rippling of the water which the ALOS-2 best illustrates.

5.5 Case 5: 2019-07-08. Level Ice

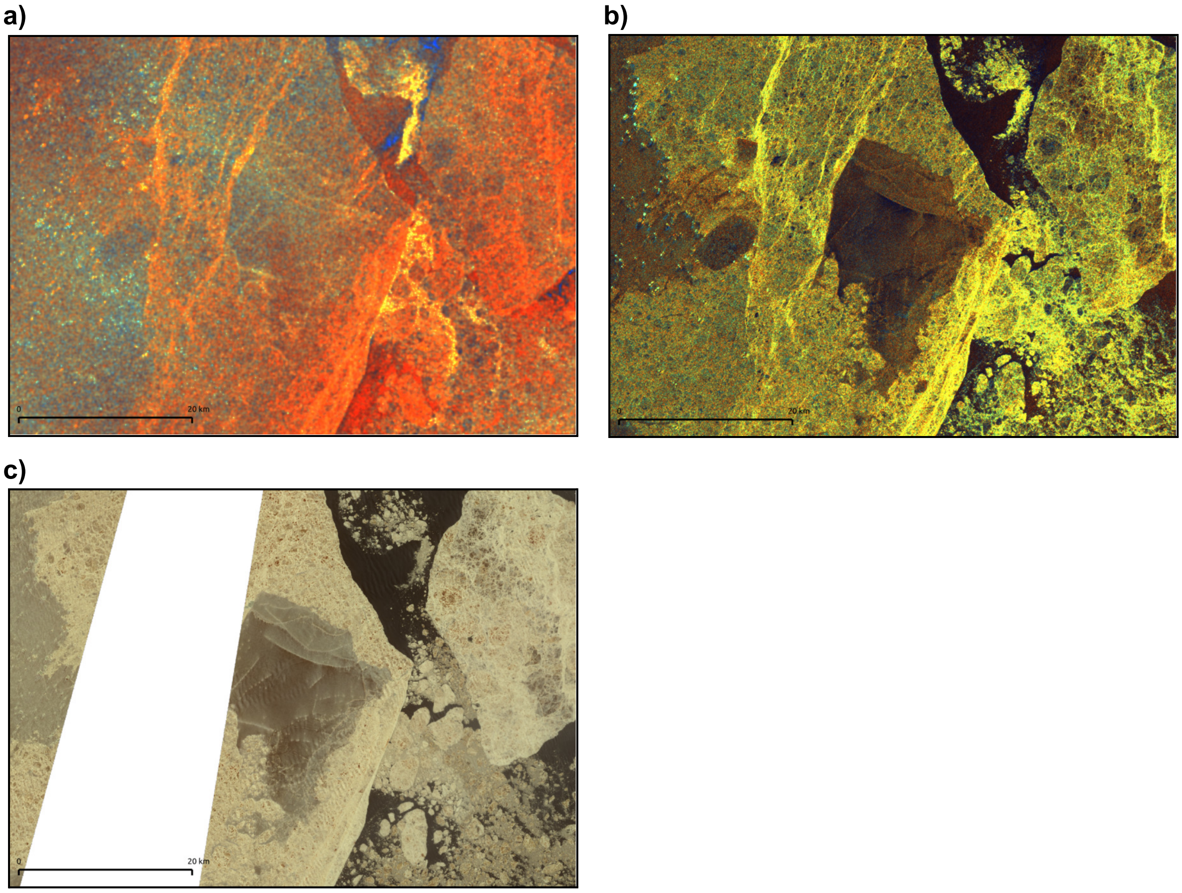

Figure 39: Case 5. a) Sentinel-1. b) ALOS-2. c) Sentinel-2.

The dark area is Interpreted as leveled ice FYI/young ice, this signature is very distinct in the ALOS-2 compared to the Sentinel-1 (Figure 39).

5.6 Case 6: 2019-09-02 Melting Conditions

a) b)

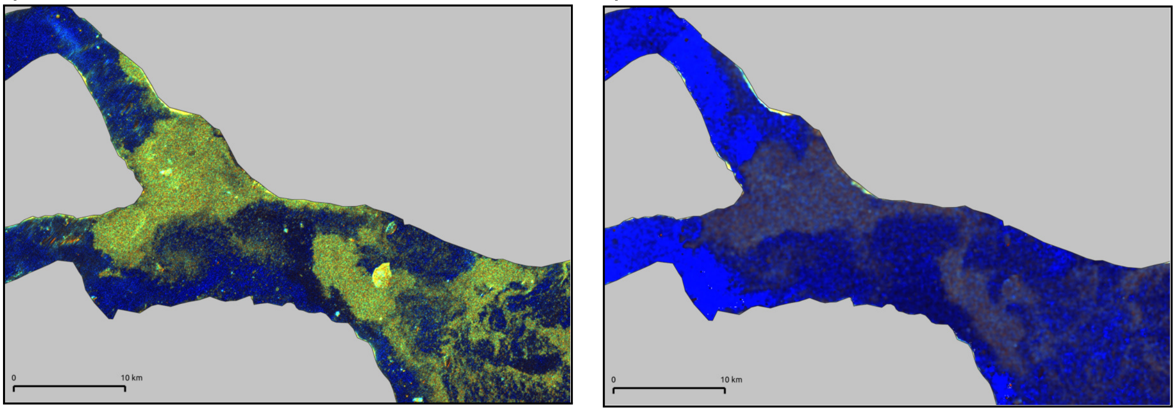

Figure 40: Case 6. a) ALOS-2. b) Sentinel-1.

Floes are easily identified in the ALOS-2 image while the signature in the Sentinel-1 image appears rather diffuse and dim (Figure 40). As the ice is in the melting stage at this time of the year this could be a situation of wet snow overlying the ice. The lower frequency of the L-band ALOS-2 better penetrates the overlying wet cover of the ice, emitting backscatter which better represents the ice signature. Similar results have been achieved by (Casey et al., 2016). The frequency of the C-band Sentinel-1 might be too high to penetrate the wet cover over the ice which results in the satellite beam bouncing off the water and emitting a rather more diffuse and dim backscatter signature.

5.7 Case 7: 2019-11-23 Sea Ice Types

a) b)

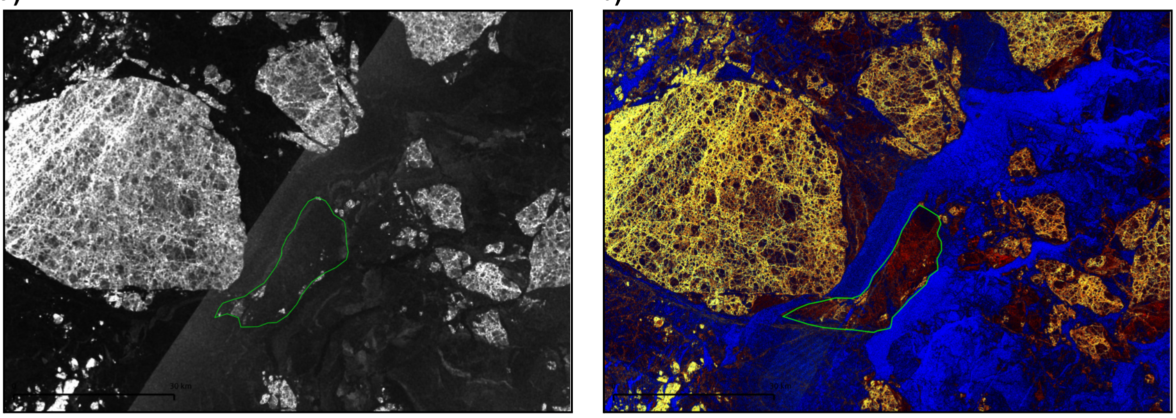

Figure 41: Case 7. a) Sentinel-1. b) ALOS-2.

The ice which is encapsulated by the green polygon in the ALOS-2 image is interpreted as young very level ice, but rougher compared to its surrounding ice, this signature is very hard to identify in the Sentinel-1 image (Figure 41).

5.8 Case 8: 2019-11-23 Level Ice

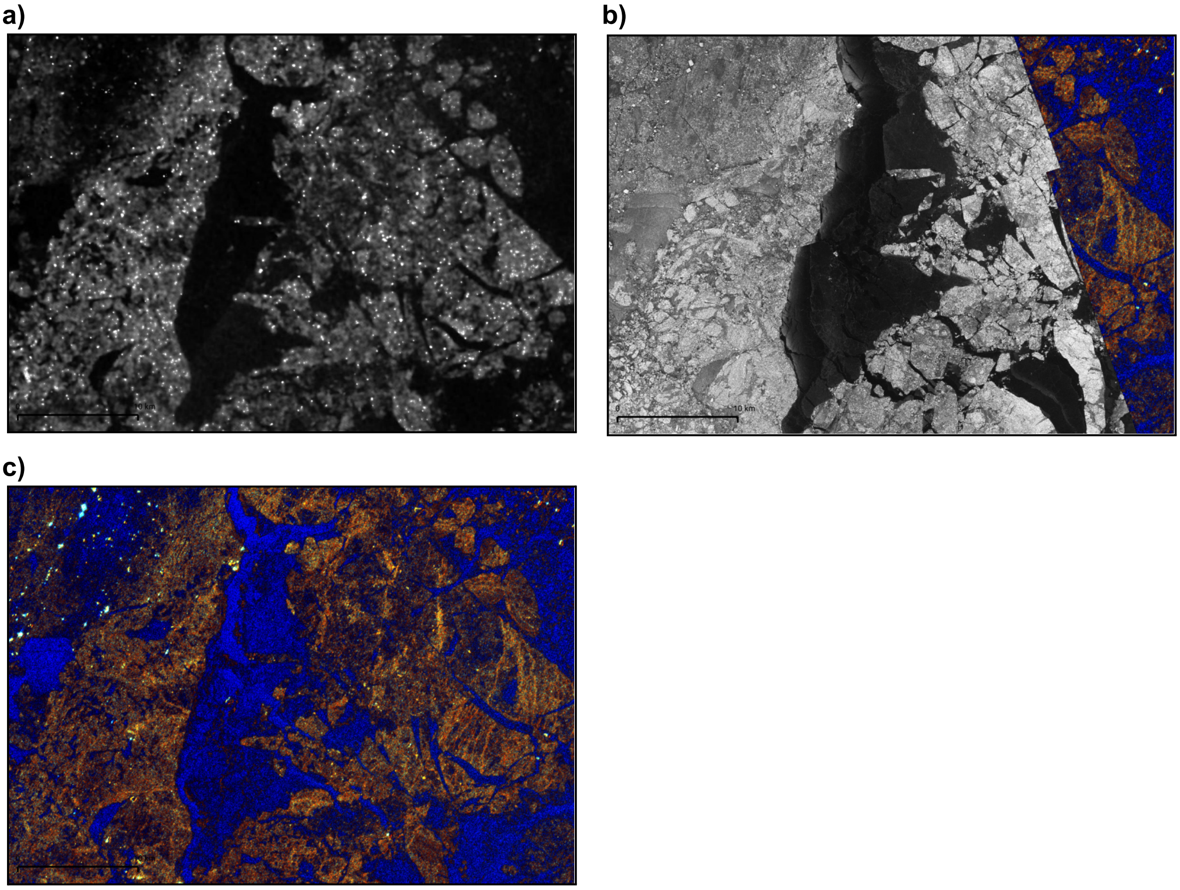

Figure 42: Case 8. a) Sentinel-1. b) COSMO-SkyMed. c) ALOS-2.

The dark uniform area is interpreted as level thin nilas ice (Figure 42a,b). The signature of this ice type is difficult to identify with the Sentinel-1 image as the image only reveals an uniform dark signature which could be misinterpreted as calm water. The CSKS however reveals thin sheet ice, which can also be seen in the ALOS-2 image (Figure 42b,c). It is worth mentioning that there is a three day time delay between the CSKS image and the two other images.

5.9 Case 9: 2019-12-09 Ridging

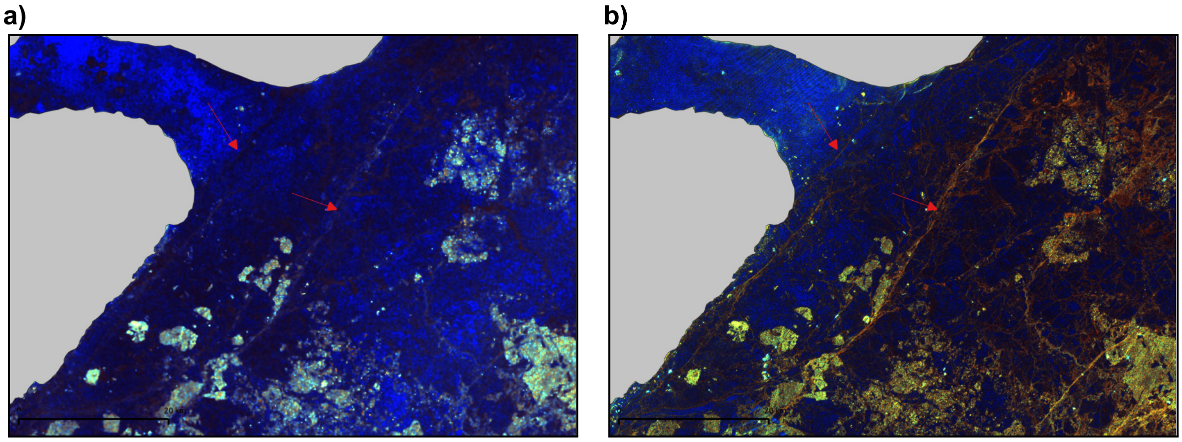

Figure 43: Case 9. a) Sentinel-1. b) ALOS-2.

Sea ice ridging is easier identified on the ALOS-2 images as they appear to reflect more backscatter than the Sentinel-1 which appears rather dim (Figure 43).

5.10 Case 10: 2019-12-09 Icebergs

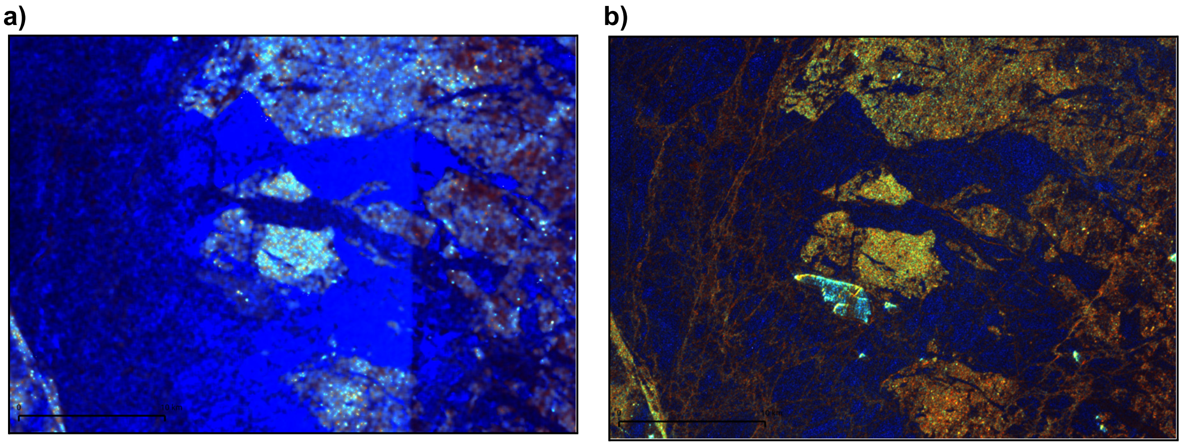

Figure 44: Case 10. a) Sentinel-1. b) ALOS-2.

The bright reflection signature identified in the ALOS-2 image is interpreted as an Iceberg, this signature does not appear in the Sentinel-1 image and this makes it very difficult to identify the iceberg in the Sentinel-1 image (Figure 44).

5.11 Case 11: 2020-02-15 Grease Ice/Frazil/Slush

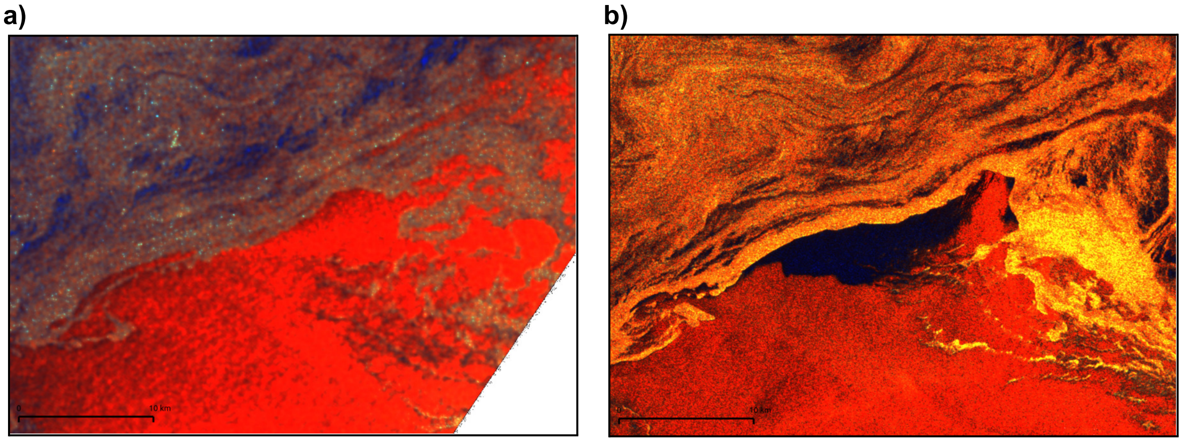

Figure 45: Case 11. a) Sentinel-1. b) ALOS-2.

The dark area has been interpreted as frazil or grease ice which causes a dampening effect on the backscatter (Figure 45b). This signature is only identified in the ALOS-2 image and not in the Sentinel-1.

5.12 Case 12: 2020-03-15 Ridging

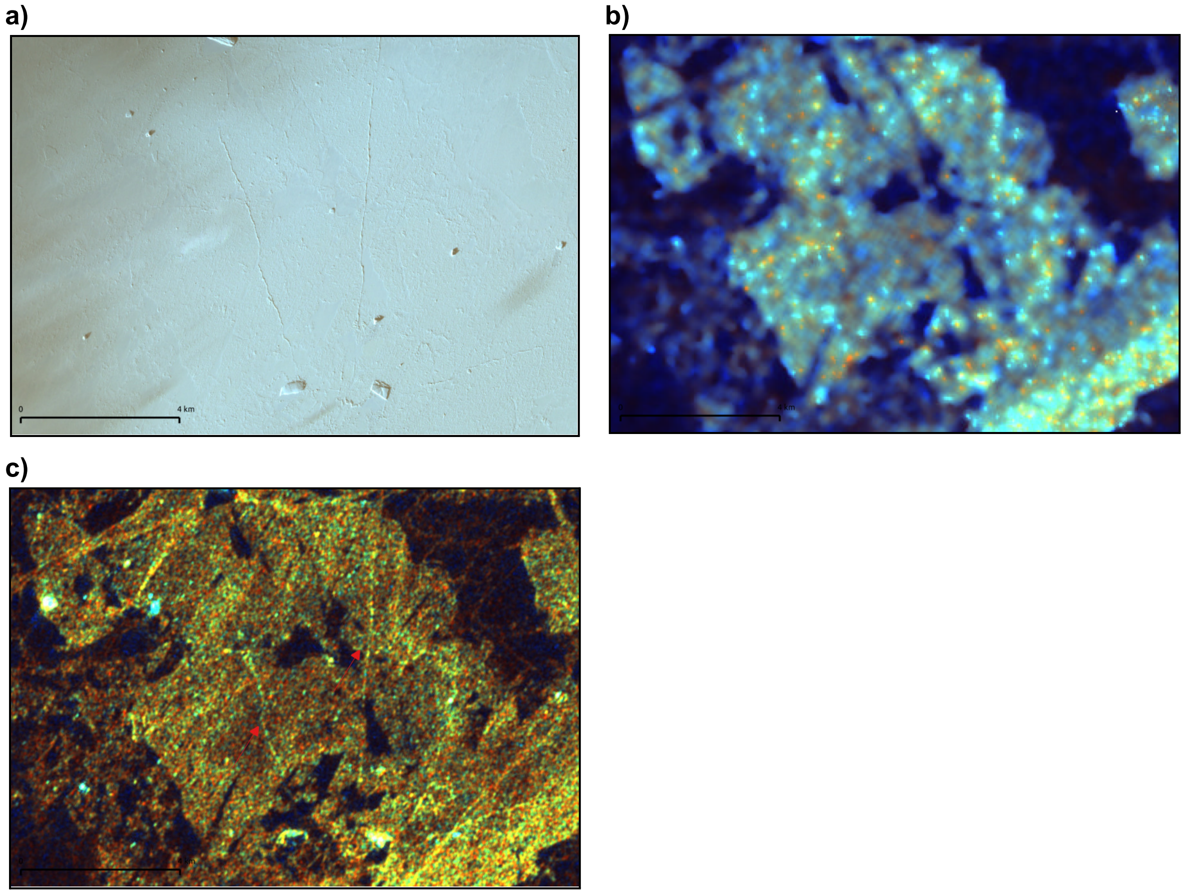

Figure 46: Case 12. a) Sentinel-2. b) Sentinel-1. c) ALOS-2.

Two stripe features identified in the Sentinel-2 and ALOS-2 images are interpreted to represent ridges (Figure 46a,c). These ridges are not identified in the Sentinel-1 image. Notice also how the two icebergs located below the ridges are present in both the Sentinel-2 and ALOS-2 images but not in the Sentinel-1 image (Figure 46).

6. Conclusion and Lessons Learned

- ALOS-2 data has proven to be very useful when it comes to identifying icebergs compared to Sentinel-1 data where the icebergs in some cases tend to be unrecognizable in situations where they are not standalone but rather present along sea ice (Case 10).
- Trying to distinguish sea ice types, ALOS-2 has also proven to be useful. In many cases the backscatter anomaly response between first-year ice and multiyear ice has had a higher contrast than for the Sentinel-1 images, making it easier to separate the two ice types (Case 2). This also goes for more leveled sea ice types such as nilas and young ice (Case 5, 7, 8). However there was one instance where the Sentinel-1 image better responded to leveled sea ice type classification (Case 1).
- ALOS-2 data seems also to be a better alternative when it comes to distinguishing between ice and water as some of the cases have better illustrated the wind effects imposed on the water compared to the Sentinel-1 images (Case 4 and Case 11).
- The lower frequency of the ALOS-2 might be better during summer season and melting stage as it better penetrates wet snow cover/water (Case 6).

7. Acknowledgements

This study is a contribution by MET Norway to the work of the Centre for Integrated Remote Sensing and Forecasting for Arctic Operations (CIRFA) and was funded through both the European Horizon 2020 research and innovation programme "*From Copernicus Big Data to Extreme Earth Analytics*" (ExtremeEarth) project (Grant Agreement 825258) and ESA "*Synergistic Use of L- and C-Band SAR Satellites for Sea Ice Monitoring*" project (Contract No. 4000130509/20/NL/FF/ab). CIRFA is one of 17 Centres for Research-based Innovation (SFI) granted in 2014 and is funded under the Research Council of Norway (RCN) project number 237906

ICESat-2 data is provided by NASA and NSIDC, see Kwok, R., A. A. Petty, G. Cunningham, T. Markus, D. Hancock, A. Ivanoff, J. Wimert, M. Bagnardi, N. Kurtz, and the ICESat-2 Science Team. 2019 and 2020. ATLAS/ICESat-2 L3A Sea Ice Freeboard, Version 5. ATL10. Boulder, Colorado USA. NSIDC: National Snow and Ice Data Center. doi: https://doi.org/10.5067/ATLAS/ATL10.005. 2019 and 2020.

FA provided the sea ice analysis dataset and initial draft of the report. NH provided overall project management, satellite data preprocessing, the iceberg analysis dataset, and final editing of this report. The authors would also like to thank Wolfgang Dierking for his proof-reading and helpful comments in the preparation of the report.

8. References

Casey, J. & Howell, Stephen & Tivy, Adrienne & Haas, Christian. (2016). Separability of sea ice types from wide swath C- and L-band synthetic aperture radar imagery acquired during the melt season. Remote Sensing of Environment. 174. 314-328. http://dx.doi.org/10.1016/j.rse.2015.12.021

Hughes, N.E., Wilkinson, J.P., & Wadhams, P. (2011). Multi-satellite sensor analysis of fast-ice development in the Norske Øer Ice Barrier, northeast Greenland. *Annals of Glaciology*, **52**(57), 151-160. https://doi.org/10.3189/172756411795931633

Jakobsson, M., Mayer, L.A., Bringensparr, C. et al. The International Bathymetric Chart of the Arctic Ocean Version 4.0. Sci Data 7, 176 (2020). https://doi.org/10.1038/s41597-020-0520-9

Kwok, R., A. A. Petty, G. Cunningham, T. Markus, D. Hancock, A. Ivanoff, J. Wimert, M. Bagnardi, N. Kurtz, and the ICESat-2 Science Team. 2019 and 2020. ATLAS/ICESat-2 L3A Sea Ice Freeboard, Version 5. ATL10. Boulder, Colorado USA. NSIDC: National Snow and Ice Data Center. doi: https://doi.org/10.5067/ATLAS/ATL10.005. 2019 and 2020.

Further information on the satellites used can be found online at:

https://sentinels.copernicus.eu/web/sentinel/missions/sentinel-1

https://sentinels.copernicus.eu/web/sentinel/missions/sentinel-2

https://www.nasa.gov/content/goddard/about-icesat-2

https://earth.esa.int/eogateway/missions/cosmo-skymed

https://www.eorc.jaxa.jp/ALOS-2/en/about/palsar2.htm